1   **Transcriptome dynamics at the *Arabidopsis* graft junction reveal an inter-tissue**

2   **recognition mechanism that activates vascular regeneration**

3

4   Charles W Melnyk[1,2], Alexander Gabel[3], Thomas J Hardcastle[4], Sarah Robinson[5],

5   Shunsuke Miyashima[6], Ivo Grosse[3], Elliot M Meyerowitz[1,7]

6

7   1- Sainsbury Laboratory, University of Cambridge, Bateman Street, Cambridge CB2

8   1LR, UK

9   2 – Department of Plant Biology, Swedish University of Agricultural Sciences, Almas

10   allé 5, 756 51 Uppsala, Sweden

11   3 - Institute of Computer Science, Martin Luther University Halle–Wittenberg, 06120

12   Halle (Saale), Germany

13   4 – Department of Plant Sciences, University of Cambridge, Downing Street,

14   Cambridge CB2 3EA, United Kingdom

15   5 - Institute of Plant Science, University of Bern, Altenbergrain 21, 3013 Bern,

16   Switzerland

17   6 – Graduate School of Biological Sciences, Nara Institute of Science and

18   Technology, 8916-5 Takayama, Ikoma, Nara 630-0192, Japan

19   7 – Howard Hughes Medical Institute and Division of Biology and Biological

20   Engineering, California Institute of Technology, 1201 East California Boulevard,

21   Pasadena, CA 91125, USA

22

23   Contact: charles.melnyk@slu.se

24

25

26

27

28

29

30

31

32

33

34

ABSTRACT

The ability for cut tissues to join together and form a chimeric organism is a remarkable property of many plants, however, grafting is poorly characterized at the molecular level. To better understand this process we monitored genome-wide temporal and spatial gene expression changes in grafted *Arabidopsis thaliana* hypocotyls. Tissues above and below the graft rapidly developed an asymmetry such that many genes were more highly expressed on one side than the other. This asymmetry correlated with sugar responsive genes and we observed an accumulation of starch above the graft that decreased along with asymmetry once the sugar-transporting vascular tissues reconnected. Despite the initial starvation response below the graft, many genes associated with vascular formation were rapidly activated in grafted tissues but not in cut and separated tissues indicating that a recognition mechanism activated that was independent of functional vascular connections. Auxin which is transported cell-to-cell, had a rapidly elevated response that was symmetric, suggesting that auxin was perceived by the root within hours of tissue attachment to activate the vascular regeneration process. A subset of genes were expressed only in grafted tissues, indicating that wound healing proceeded via different mechanisms depending on the presence or absence of adjoining tissues. Such a recognition process could have broader relevance for tissue regeneration, inter-tissue communication and tissue fusion events.

INTRODUCTION

For millennia people have cut and rejoined plants through grafting. Generating such chimeric organisms combines desirable characteristics from two plants, such as disease resistance, dwarfing and high yields, or can propagate plants and avoid the delays entailed by a juvenile state (1). Agriculturally, grafting is becoming more relevant as a greater number of plants and species are grafted to increase productivity and yield (2). However, our mechanistic understanding of grafting and the biological processes involved, including wound healing, tissue fusion and vascular formation, remain limited.

Plants have efficient mechanisms to heal wounds and cuts, in part through the production of wound-induced pluripotent cells termed callus. The callus fills the gap

69 or seals the wound, and later, differentiates to form epidermal, mesophyll and

70 vascular tissues (3). In grafted *Arabidopsis* hypocotyls, tissues adhere 1-2 days after

71 grafting and the phloem, the tissue that transports sugars and nutrients, connects after

72 three days (4, 5). The xylem, tissue that transports water and minerals, connects after

73 seven days (4). Plant hormones are important regulators of vascular formation, and at

74 the graft junction, both auxin and cytokinin responses increase in the vascular tissue

75 (4-6). Auxin is important for differentiation of vascular tissues whereas cytokinin

76 promotes vascular stem cells, termed cambium, to divide and proliferate in a process

77 known as secondary growth (7, 8). Auxin is produced in the upper parts of a plant and

78 moves towards the roots via cell-to-cell movement. Auxin exporters, including the

79 PIN proteins, transport auxin into the apoplast, whereas auxin importers, such as the

80 AUX and LAX proteins, assist with auxin uptake into adjacent cells (8). Disrupting

81 this transport, such as by mutating *PIN1*, inhibits healing of a wounded stem (9).

82 Blocking auxin transport with the auxin transport inhibitor TIBA (2,3,5-

83 triiodobenzoic acid) in the shoot inhibits vascular formation and cell proliferation at

84 the *Arabidopsis* graft junction (6). In addition to auxin, other compounds, including

85 sugars, contribute to vascular formation. The localised addition of auxin to callus

86 induces phloem and xylem but requires the presence of sugar (10, 11). In plants,

87 sugars are produced in the leaves and transported through the phloem to the roots

88 (12). The role of sugars in vascular formation and wound healing is not well

89 established, however, sugars promote cell division and cell expansion (13), processes

90 important for development including vascular formation.

91

92 The molecular and cellular mechanisms for wound healing, tissue reunion and graft

93 formation remain largely unknown. One emerging theme is that the top and bottom of

94 the cut do not behave similarly. Such tissue asymmetry occurs in other plant tissues,

95 most notably leaves. Developing leaf primordia have an inherent asymmetry that is

96 thought to derive from positional signals from the shoot apical meristem that specifies

97 differences between the top and the bottom of the leaf. The molecular mechanisms

98 that establish asymmetry are not well described, though one hypothesis is that auxin

99 contributes towards or acts on the putative signal (14). Asymmetry also appears in cut

100 *Arabidopsis* inflorescence stems where the transcription factor *RAP2.6L* expresses

101 exclusively below the cut whereas the transcription factor *ANAC071* expresses

102 exclusively above the cut (9). Both were important for stem healing and *ANAC071*

103 and a close homologue, *ANAC096,* were important for graft formation (6).

104 Asymmetry also exists in genetic requirements, since *ALF4* and *AXR1*, two genes

105 involved in auxin perception, are important below but not above the graft junction for

106 phloem connection (4). However, *ANAC071* is expressed symmetrically around the

107 hypocotyl graft junction three days after grafting (6) so the extent of asymmetry and

108 the mechanistic basis for it during wound healing remains largely uncharacterised.

109

110 Previous efforts have characterised wound healing and tissue reunion using

111 transcriptomic analyses. Mechanical wounding altered approximately 8% of the

112 *Arabidopsis* transcriptome and showed a high degree of overlap with transcriptomic

113 changes elicited by pathogen attack and abiotic stress (15). Stem wounding and

114 wound-induced callus formation altered the expression of hundreds or thousands of

115 genes (9, 16, 17), whereas grafting grape vines, lychee trees and hickory trees induced

116 hundreds or thousands of differentially expressed genes involved in hormone

117 response, wound response, metabolism, cell wall synthesis and signal transduction (5,

118 18-21). These grafting studies provide limited information, as tissues from above and

119 below the graft junction were not isolated to test whether these tissues behaved

120 differently, and controls were not performed to distinguish how grafting and tissue

121 fusion might differ from a response associated with cut tissues that remained

122 separated. Here, we perform an in-depth analysis to describe the spatial and temporal

123 transcriptional dynamics that occur during healing of cut *Arabidopsis* tissues that are

124 joined (grafted) or left unjoined (separated). We find that the majority of genes

125 differentially expressed are initially asymmetrically expressed at the graft junction

126 and that many of these genes are sugar responsive, which correlates with severing of

127 the phloem tissue and the accumulation of starch above the junction. However, genes

128 associated with cell division and vascular formation activate on both sides of the graft

129 and, similarly, auxin responsiveness activates equally on both sides. We propose that

130 the continuous transport of substances, including auxin, independent of functional

131 vascular connections, promoted division and differentiation, while the enhanced auxin

132 response and blocked of sugar transport provided a unique physiological condition to

133 activate genes specific to graft formation that promote wound healing.

134

135 **RESULTS**

136 **Genes are asymmetrically expressed around the graft**

137   Previous analyses revealed an asymmetry in several genes important for tissue

138   reunion or graft formation and identified a number of genes expressed above a cut

139   that were not expressed below (4, 9). To investigate whether asymmetry was a

140   common feature of grafting and tissue reunion, we generated RNA deep sequencing

141   libraries from *Arabidopsis thaliana* hypocotyl tissues immediately above and

142   immediately below the graft junction 0, 6, 12, 24, 48, 72, 120, 168 and 240 hours after

143   grafting (HAG)(Figure 1A). Prior to RNA extraction, we separated top and bottom

144   tissues at the graft junction. We found that the strength required to break apart the

145   graft junction increased linearly (Figure S1) similarly to previously reported breaking

146   strength dynamics of grafted *Solanum pennellii* and *Solanum lycopersicum* (22, 23).

147   When pulling apart grafts to separate top and bottom for sample preparation, grafts

148   broke cleanly with minimal tissue from one half present in the other half (Figure S1,

149   Movie S1, S2). We measured the amount of tissue from tops adherent to bottoms and

150   *vice versa* (Figure S1) and found less than 4% cross-contamination. In addition to

151   grafting, we also prepared libraries from ungrafted hypocotyls ("intact" treatment)

152   and cut plants that had not been reattached ("separated" treatment)(Figure 1A). We

153   herein refer to tissues harvested above the graft junction or from the shoot side of

154   separated tissue as "top" and that from below the graft or from the root side of

155   separated tissue as "bottom" (Figure 1A).

156

157   RNAs that were differentially expressed as a consequence of grafting (compared to

158   intact hypocotyls) equally in tops and bottoms of grafts (symmetrically expressed) or

159   were more highly expressed in one tissue than the other (asymmetrically expressed),

160   were identified by performing a pairwise analysis of the protein-coding transcriptome

161   datasets that were differentially expressed relative to the intact group. Several

162   thousand RNAs were identified that fit either pattern of expression including the

163   transcript of the cambial markers *HCA2* that was induced symmetrically, and *ANT*

164   that was induced asymmetrically (Figure 1B-G, Figure S2). 6 to 48 hours after

165   grafting, the number of graft-differentially expressed genes that were asymmetrically

166   expressed was roughly 3-fold greater than those symmetrically expressed indicating

167   that tissues above the cut changed their expression dynamics relative to below the cut.

168   However, at 72 hours the numbers were nearly equal, and by 120 hours, the number

169   of symmetrically differentially expressed genes was 3-fold greater than those

170   asymmetrically expressed (Figure 1B). As a second approach, we performed a

171   hierarchical clustering analysis that indicated that the grafted top and grafted bottom

172   became most similar after 72 hours (Figure S3), consistent with the symmetry

173   analysis (Figure 1B). Thus, graft healing and tissue reunion promoted a shift from

174   asymmetry to symmetry (Figure 1B).

175

176
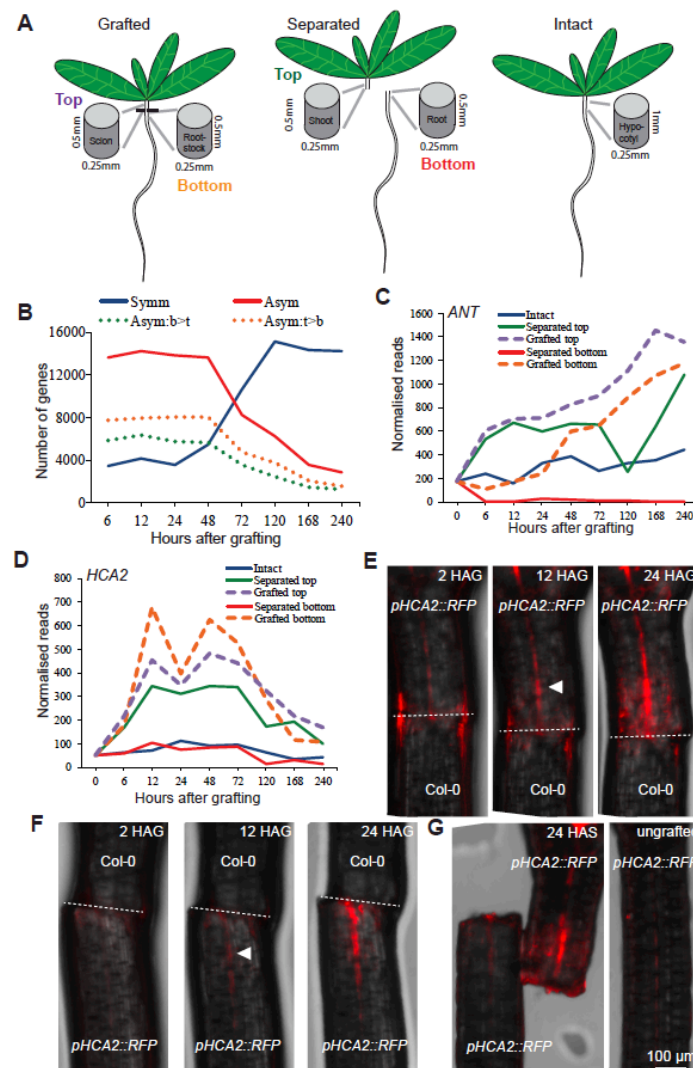
177   **Figure 1. Grafting rapidly activates genes in both asymmetric and symmetric**
178   **patterns.** (A) Intact, cut and separated, or cut and grafted *Arabidopsis* tissues were
179   harvested approximately 0.5mm above (top), 0.5mm below (bottom) the cut site or for
180   intact plants 1mm segments spanning the region where cuts were made in grafted and
181   separated plants. (B) Pairwise analysis between the grafted top and grafted bottom
182   identified sets of protein-coding genes symmetrically or asymmetrically expressed at
183   the graft junction, with an FDR < 0.05 and a likelihood of symmetric/asymmetric
184   expression of greater than 50%. Asymmetrically expressed genes were further divided
185   into those whose RNAs were higher in the top (orange dotted line) or higher in the
186   bottom (purple dotted line), again with an FDR < 0.05 and a likelihood of asymmetric
187   expression greater than 50%. (C,D) Expression profiles for transcripts of cambium-
188   associated genes that initially activate symmetrically (*HCA*) or asymmetrically (*ANT*)
189   plotted for intact, separated and grafted samples. (E-G) *HCA2* transcription

190 upregulates above the graft junction (E) and below the graft junction. (F)
191 *pHCA2::RFP* was grafted to Col-0 roots (E) or Col-0 shoots (F) to avoid ambiguity of
192 signal origin at the junction. *HCA2* was also upregulated in separated shoots but not in
193 intact samples or in high levels in separated roots (G). HAG, hours after grafting.
194 HAS, hours after separation. White triangle denotes initial fluorescent signal, dashed
195 lines denote the graft junction.

196
197 **Sugar response correlates with asymmetric gene expression**
198 The shift from asymmetry to symmetry could be due to phloem reconnection at 72
199 hours ((4), Figure 2A) and the resumption of hormone, protein and sugar transport.
200 We tested a role for sugar by grafting in the presence of exogenous sucrose which has
201 previously been reported to affect grafting success (24). Low levels of exogenous
202 sucrose lowered grafting efficiency (Figure 2A), suggesting that differential sugar
203 responses at the graft junction might be important for vascular reconnection.
204 Expression of *ApL3*, a gene whose expression is induced by sugar (25), was rapidly
205 upregulated in separated tops and grafted tops, whereas expression of *DIN6*, *GDH1*
206 and *STP1*, genes whose expression is repressed by sugar (25-27), was rapidly
207 upregulated in separated bottoms and grafted bottoms (Figure 2B, Figure S4). These
208 observations were consistent with sugar accumulation in the grafted top and sugar
209 depletion in the grafted bottom. The expression of these genes returned to levels
210 similar to intact samples by 120 hours and, with the exception of *ApL3*, the grafted
211 samples normalised expression more rapidly than the separated tissues. Genes
212 associated with photosynthesis increase expression in separated bottoms 24 hours
213 after cutting, a common response to starvation (13), but likely too late to affect sugar
214 levels before 24 hours (Figure S4). A transcriptional overlap analysis with RNAs
215 from known glucose-responsive genes (Table S1) revealed a strong overlap with
216 genes differentially expressed by grafting. RNAs from known glucose-induced genes
217 were upregulated in separated tops and grafted tops, whereas transcripts from known
218 glucose-repressed genes were upregulated in separated bottoms and grafted bottoms
219 (Figure 2C, Figure S4). This trend was not observed with genes differentially
220 expressed by mannitol treatment (Figure S4), suggesting the effect was specific to
221 metabolically active sugars. To further investigate this effect, we stained grafted,
222 separated and intact plants with Lugol solution to assay for the presence of starch.
223 Staining above the graft junction increased 48-72 hours after grafting (Figure 2D). By
224 120 hours, staining was equal on both sides of the graft whereas in separated tops
225 staining became stronger after 72 hours (Figure 2D, Figure S4). We concluded that

226   starch accumulated above the graft junction, but after 72 hours, this asymmetry

227   disappeared. To test whether the accumulation of starch and increased sugar

228   responsiveness could explain the observed transition from asymmetry to symmetry,

229   we compared our datasets to previously published genes that are induced by

230   starvation or are induced by sucrose re-addition (Table S1). In early time points, 20-

231   31% of asymmetrically expressed genes are genes known to respond to sugars

232   compared to 2-5% of symmetrically expressed genes (Table 1). However, at 72 hours,

233   the overlap between asymmetrically expressed genes and sugar responsive genes

234   reduced substantially (Table 1).

235
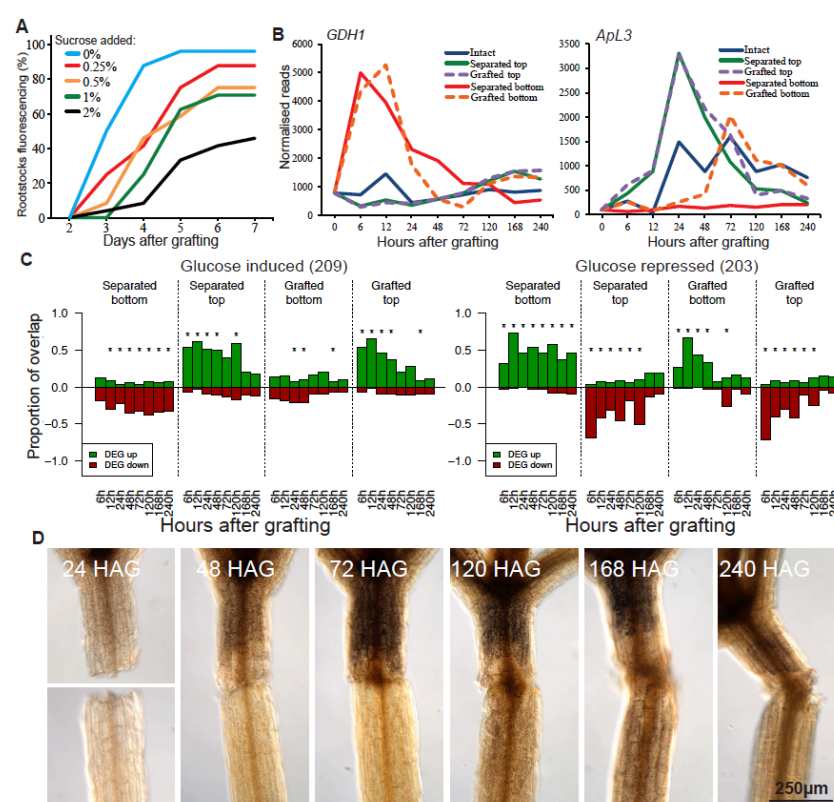
236   **Figure 2. Asymmetric changes in accumulation of sugar-responsive RNAs and of**
237   **starch occur at the graft junction; equalizing sucrose between the grafted**
238   **segments reduces and delays phloem reconnection.** (A) *pSUC2::GFP*-expressing
239   *Arabidopsis* shoots were grafted to Col-0 wild type roots and GFP movement to the
240   roots was monitored over 7 days for phloem connection in the presence or absence of
241   various concentrations of sucrose. (B) Expression profiles for transcripts of a sugar-
242   repressed gene (*GDH1*), and a sugar-induced gene (*ApL3*) were plotted for intact,
243   separated and grafted samples. (C) Transcriptional overlap between previously
244   published glucose-induced or glucose repressed genes and our dataset. The number in
245   brackets represents the number of glucose-responsive genes identified in the previous
246   dataset, and overlap is presented as a ratio out of 1.0 for differentiation expressed
247   genes (DEG) up- or down-regulated in our dataset relative to intact samples. Asterisks
248   represent a significant difference (p < 0.05) between the ratio of up- and down-
249   regulated genes in a previously published transcriptome dataset compared to the ratio

250 of all up- and down- regulated genes in our grafting dataset at a certain time point. (D)
251 Lugol staining of grafted plants at various time points revealed dark brown staining
252 associated with starch accumulation. HAG, hours after grafting.
253

254 **Table 1. Sugar response overlaps with asymmetry.** Symmetrically and
255 asymmetrically differentially expressed genes were compared to previously published
256 sugar-responsive genes (28)[1] and the percent overlap calculated (* p<.05). HAG,
257 hours after grafting.
258

HAG	Sugar Induced[1]	Graft Bottom=Top	Overlap	%	Graft Top>Bottom	Overlap	%	Graft Bottom>Top	Overlap	%
6	2243	4988	263	5	6679	1403	21*	4971	99	2
12	2243	3473	165	5	7111	1444	20*	5657	231	4
24	2243	4135	171	4	6873	1414	21*	4942	195	4
48	2243	3689	197	5	6601	1241	19*	4915	218	4
72	2243	10421	1005	10*	2459	228	9*	2019	138	7
120	2243	15012	1063	7	1510	220	15*	941	115	12*

HAG	Sugar Repressed[1]	Graft Bottom=Top	Overlap	%	Graft Top>Bottom	Overlap	%	Graft Bottom>Top	Overlap	%
6	1998	4988	107	2	6679	53	1	4971	1563	31*
12	1998	3473	68	2	7111	112	2	5657	1526	27*
24	1998	4135	88	2	6873	72	1	4942	1525	31*
48	1998	3689	113	3	6601	93	1	4915	1427	29*
72	1998	10421	530	5	2459	111	5	2019	538	27*
120	1998	15012	979	7	1510	84	6	941	210	22*

259
260

261 **Vascular formation and cell division activates on both sides of the graft**

262 Since the grafted bottom samples exhibited a starvation response up to 48 hours after

263 grafting, we reasoned that pathways associated cell division and cell differentiation

264 would be delayed or inhibited. We looked at the expression of markers associated

265 with vascular formation and cell division in the transcriptome datasets. Cambium,

266 phloem and provascular markers activated within 6 hours in grafted top samples, but

267 activation was only delayed 0-24 hours in grafted bottom samples depending on the

268 gene (Figure 1B-C, Figure 3, Figure S5, Figure S6). Expression of phloem markers

269 peaked in both grafted tops and grafted bottoms at 72 hours (Figure 3, Figure S5,

270 Figure S6), the time when phloem reconnections form in grafted *Arabidopsis* (Figure

271 1, (4, 5)). Notably, the early phloem marker *NAC020* activated before the mid phloem

272 marker *NAC086* which activated before the late phloem marker *NEN4*, consistent

273 with the dynamics of phloem transcriptional activation during primary root

274 development and leaf vascular induction (Figure S5)(29, 30). Certain markers

275 associated with xylem formation, such as *VND7* and *BFN1*, activated early in the

276 grafted top. Other xylem markers, such as *IRX3* and *CESA4*, activated late in grafted

277 samples. By 120 hours after grafting, xylem markers were activated in top and

278 bottom, consistent with when the first xylem strands differentiate at the graft junction

279   (4). Genes associated with cell division were activated by 12 hours in the grafted top

280   and by 24 hours in the grafted bottom (Figure 3, Figure S5). On the other hand,

281   control genes whose expression does not typically vary between tissues and

282   treatments (31) were not differentially expressed in grafted tops or bottoms (Figure

283   S6). The RNAseq expression data appeared to correlate well with transcriptional

284   fluorescent reporters for both activation dynamics and the localisation of expression

285   (Figure 1D-F, Figure S2).

286

287   The similar activation dynamics of vascular differentiation genes in grafted tops and

288   grafted bottoms prompted us to test whether this phenomenon occurred with other

289   known developmental processes. We obtained lists of genes whose expression is

290   associated with various biological processes from previous publications (Table S1)

291   and tested how many of the genes differentially expressed in our transcriptomes

292   overlapped with the previously published lists. Differentially expressed genes in

293   grafted samples and separated tops partially overlapped with those whose expression

294   is associated with phloem, xylem and procambium formation (Figure 4, Figure S7).

295   There was a high overlap between *Arabidopsis* inflorescence stem healing and

296   grafting, as well as between vascular induction in leaf disk cultures and grafting

297   (Figure 4). Various genes expressed in a cell type-specific manner also showed a high

298   transcriptional overlap with grafting, including phloem, endodermis and protoxylem

299   (Figure 4, Figure S7). In nearly all cases, the separated top, grafted top and grafted

300   bottom samples showed similar activation dynamics. The separated bottom samples

301   were exceptional though since gene expression associated with vascular development

302   and cell-specific processes was downregulated (Figure 4, Figure S7). We also

303   compared our datasets to RNAs expressed in longitudinal cross sections of the

304   *Arabidopsis* root (32). There was little overlap between grafted bottoms and sections

305   from the root meristemic zone, whereas overlap existed between grafted tops and the

306   root meristemic zone in early time points, and between grafting and the root

307   maturation zone (Figure S8). Our analysis also revealed that two genes expressed in

308   cambium, *WOX4* and *PXY*, were induced by grafting but the primary root marker

309   *WOX5* and lateral root marker *LBD18* were not (Figure 3, Figure S5, Figure S6).
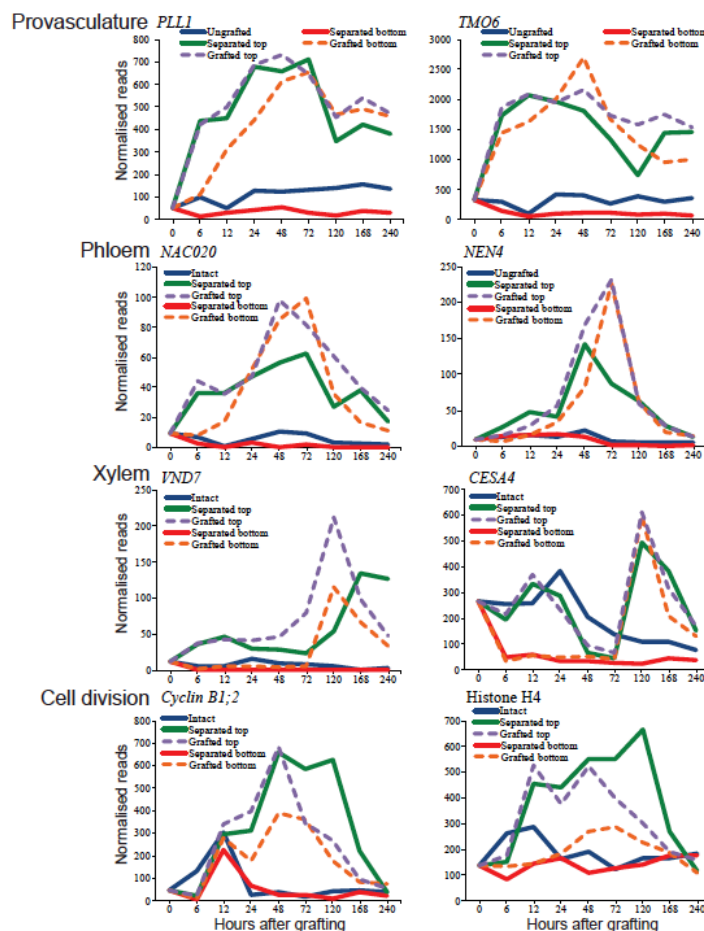
Figure 3. Transcriptional dynamics of genes associated with provasculature, phloem, xylem and cell division. Expression levels were plotted over time for intact, separated and grafted samples.
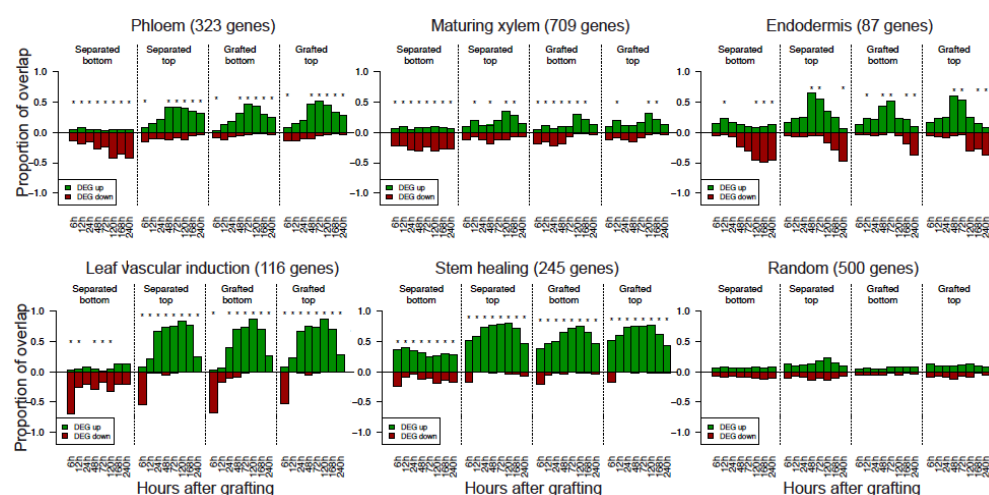

Figure 4. Transcriptional overlap between previously published vascular datasets and the grafting datasets. Genes whose transcripts are associated with various cell types or biological processes were taken from previously published datasets (see Table S1) and compared to the transcriptomic datasets generated here. The number in brackets represents the number of cell type-specific or process-specific genes identified in the previous dataset, and overlap is presented as a ratio out of 1.0

322 for differentiation expressed genes (DEG) up- or down-regulated in our dataset
323 relative to intact samples. Asterisks represent a significant difference ($p < 0.05$)
324 between the ratio of up- and down- regulated genes in a previously published
325 transcriptome dataset compared to the ratio of all up- and down- regulated genes in
326 our grafting dataset at a certain time point.

327

328 **Auxin response is symmetric at the graft**

329 The rapid activation of vascular markers in the grafted bottoms despite the starvation

330 response promoted us to investigated whether other mobile substances such as

331 phytohormones could play a role in gene activation. We compared lists of genes

332 known to respond to cytokinin, ethylene or methyl jasmonate (33) and found no

333 substantial overlap between these lists and genes differentially expressed by grafting

334 (Figure S9)(Table S1). Abscisic acid-responsive and brassinosteroid-responsive genes

335 showed overlap with genes differentially expressed in our datasets, but this overlap

336 was of a similar magnitude in both separated and grafted datasets suggesting the

337 effect was not specific to grafting (Figure S9). Auxin responsive transcripts were

338 exceptional though, as they showed a substantial overlap with RNAs differentially

339 expressed in our data sets that varied depending on the treatment (Figure 5A-B,

340 Figure S9). Auxin-induced genes were upregulated in separated tops, grafted bottoms

341 and grafted tops whereas they were repressed in separated bottoms (Figure 8). Auxin

342 responsive genes such as *IAA1* and *IAA2* (34) were induced to similar levels in grafted

343 tops and grafted bottoms at 24 hours. To further investigate whether auxin response

344 was uniform between grafted tops and grafted bottoms, we grafted the auxin-

345 responsive fluorescent reporter *p35S:DII-Venus* whose fluorescent protein is degraded

346 in the presence of auxin (35). DII-Venus fluoresced in the separated bottoms but did

347 not fluoresce in grafted bottoms 14 hours after cutting (Figure 5C) indicating

348 separated bottoms had a low level of auxin response but grafted tops, grafted bottoms

349 and separated tops had a high level of auxin response.

350
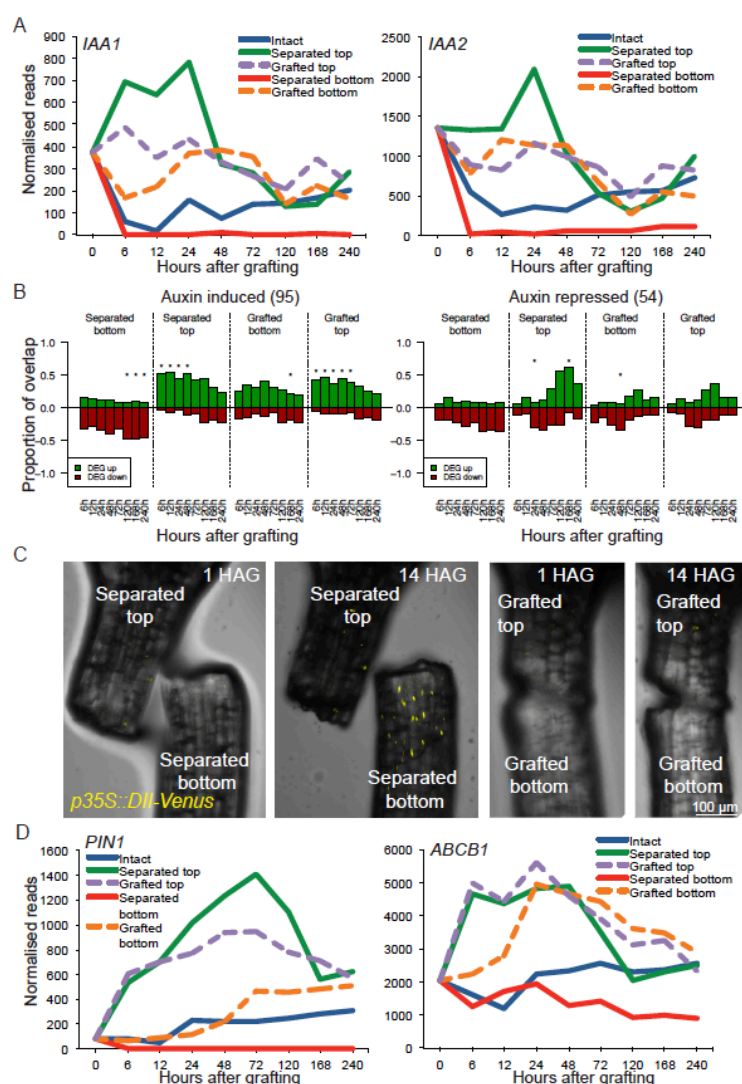
Figure 5. Auxin response is symmetric at the graft junction. (A,D) Expression profiles for various auxin-responsive genes (*IAA1*, *IAA2*) or auxin transporter genes (*PIN1* and *ABCB1* genes) were plotted for intact, separated and grafted samples. (B) Overlap between previously published auxin-induced or auxin-repressed RNAs and our dataset. The number in brackets represents the number of auxin-responsive genes identified in the previous dataset, and overlap is presented as a ratio out of 1.0 for differentiation expressed genes (DEG) up- or down-regulated in our dataset relative to intact samples. Asterisks represent a significant difference (p < 0.05) between the ratio of up- and down- regulated genes in a previously published transcriptome dataset compared to the ratio of all up- and down- regulated genes in our grafting dataset at a certain time point. (C) Grafted and separated plants expressing the auxin responsive *p35S::DII-Venus* transgene that is degraded in the presence of auxin reveal a reduction of auxin response in cut bottoms, but not in grafted bottoms. HAG, hours after grafting.

368 **Tissue fusion imparts a unique physiological response that differs from tissue**

369 **separation**

370 We hypothesized that the symmetric auxin response and asymmetric sugar response at

371 the graft junction could allow a unique transcriptional response since neither

372 separated plants nor intact plants had similar response dynamics to sugars and auxin

373 as measured by genome-wide gene response, starch accumulation and *p35S::DII-*

374 *Venus* expression (Figure 2, Figure 5). To uncover protein-coding genes differentially

375 expressed specifically by grafting, we performed an empirical Bayesian analysis (36)

376 where at each time point we computed likelihoods for each gene for each possible

377 pattern of differential expression in the intact, grafted top, grafted bottom, separated

378 top and separated bottom tissues (Figure 6A). These likelihoods were used to define a

379 similarity score between pairs of genes, which was used to cluster genes with similar

380 patterns of gene expression across the five tissues (37). Clusters were then identified

381 by the predominant pattern of gene expression observed within a cluster. This analysis

382 produced 113 clusters containing at least 10 RNAs at a single time point (Table S2;

383 Dataset S1). Approximately 6000 genes were differentially expressed in at least one

384 tissue whereas between 1000 and 4000 genes were not differentially expressed

385 (Figure 6B).

386

387 To simplify the analysis, we considered clusters where gene expression was grouped

388 into patterns consisting of one comparison. At early time points, the cluster containing

389 genes differentially expressed in grafted tops, grafted bottoms, separated tops and

390 separated bottoms had high numbers that decreased with time and could represent an

391 general wound response (Figure 6C). Similarly, clusters containing separated tops and

392 grafted tops and clusters containing separated bottoms and grafted bottoms initially

393 had high numbers that decreased with time. This observation indicated the grafted top

394 was initially transcriptionally similar to the separated top, whereas the grafted bottom

395 was initially transcriptionally similar to the separated bottom. After the 48-hour time

396 point, clusters containing genes only differentially expressed in separated tops or only

397 differentially expressed in separated bottoms increased in numbers, suggesting these

398 tissues gained a unique pattern of gene expression. The cluster containing genes

399 differentially expressed in grafted tops and grafted bottoms increase in numbers

400 throughout the healing process (Figure 6C). We searched for cluster categories that

401 contained genes only differentially expressed by grafting and found very few genes

402   downregulated by grafting or upregulated only in the grafted top (Figure 7A). Instead,

403   there were clusters that contained several hundred differentially expressed genes

404   present either in the grafted bottom only, or present in both grafted bottom and grafted

405   top (Figure 7A). Genes whose expression changed only in the grafted bottom sample

406   were prevalent early during grafting and were most common at 48 hours, whereas

407   genes activated in both top and bottom became prevalent at 48 hours and were most

408   common at 120 hours (Figure 7A). We performed a gene ontology (GO) analysis on

409   the genes whose expression was grafting-specific and found that genes coding for

410   RNAs differentially expressed only in the grafted bottom sample were enriched in the

411   immune response and chitin response biological process categories (Table S3).

412   Previously published chitin-induced RNAs had a high proportion of overlap with

413   differentially expressed graft bottom-specific genes (Figure 7E, Figure S10).

414   Grafting-specific RNAs expressed symmetrically, in both the grafted top and grafted

415   bottom, were enriched in vascular-related biological processes (Table S3). Previously

416   published phloem-enriched, endodermal-enriched, vascular-induction and stem-

417   wounding associated RNAs had a high proportion of overlap with differentially

418   expressed graft-specific genes (Figure 7C-D, Figure S10). Since few genes were

419   grafting-specific and grafted tissues were initially transcriptionally quite similar to

420   separated tissues (Figure 6C, Figure 7A), we reasoned that tissues separated for short

421   periods (<48 hours) could be grafted with similar reconnection dynamics as tissues

422   that had been grafted immediately. To test this hypothesis, plants were cut at day 0,

423   and grafted at 1-5 days after separation. Separated tissues did not speed up vascular

424   reconnection, and instead, it always took three days from the point of tissue

425   attachment for vascular connections to form (Figure S10). Furthermore, the shoot lost

426   competence to graft 2-3 days after separation whereas the root remained competent to

427   graft up to 5 days after separation (Figure S10). Together, it appears the grafted shoot

428   and root have a unique physiological response that differ from separated plants and

429   that tissue attachment is required to activate graft formation and tissue fusion.
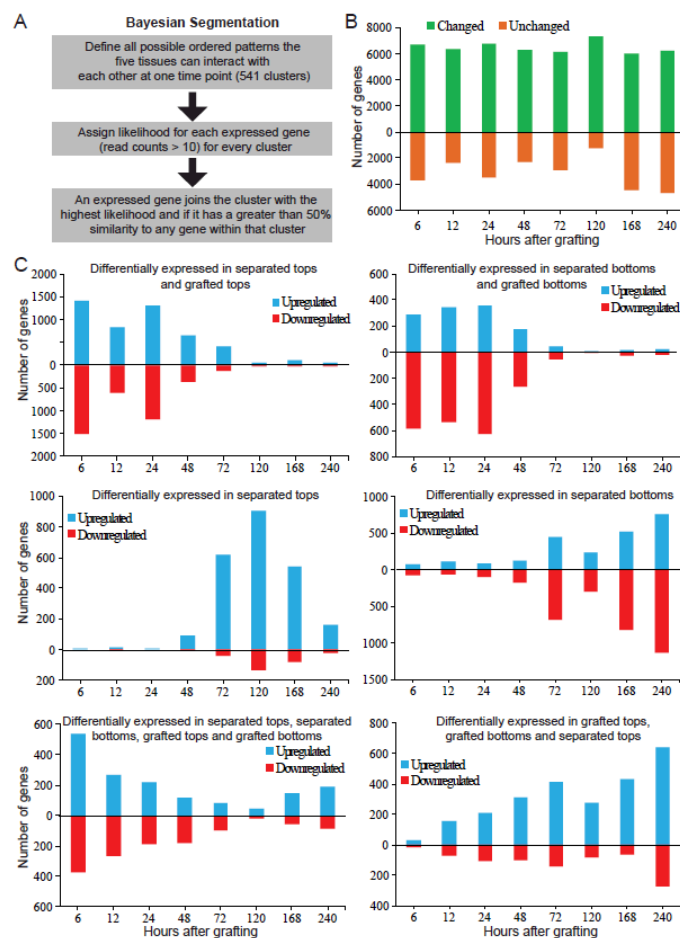
Figure 6. Clustering the transcriptome at each time point, based on likelihoods of all possible patterns of differential expression. (A) Cartoon depicting the Bayesian segmentation. (B) Analysis of differential behaviour produced 113 categories containing at least 10 genes whose expression was expressed in a specific differential pattern in at least one time point (see Table S2). One group is comprised of genes whose transcript levels are not substantially changed in the five tissues (unchanged) whereas the other group is comprised of the sum of the other 112 groups (genes whose transcript levels changed after treatment in a least one tissue) over the time points tested. (C) Major categories in the segmentation revealed RNAs whose levels changed in all the treatments listed relative to intact samples. Note that a gene can be represented only in one category for a given time point, that category in which the transcript level changes best fit the category.
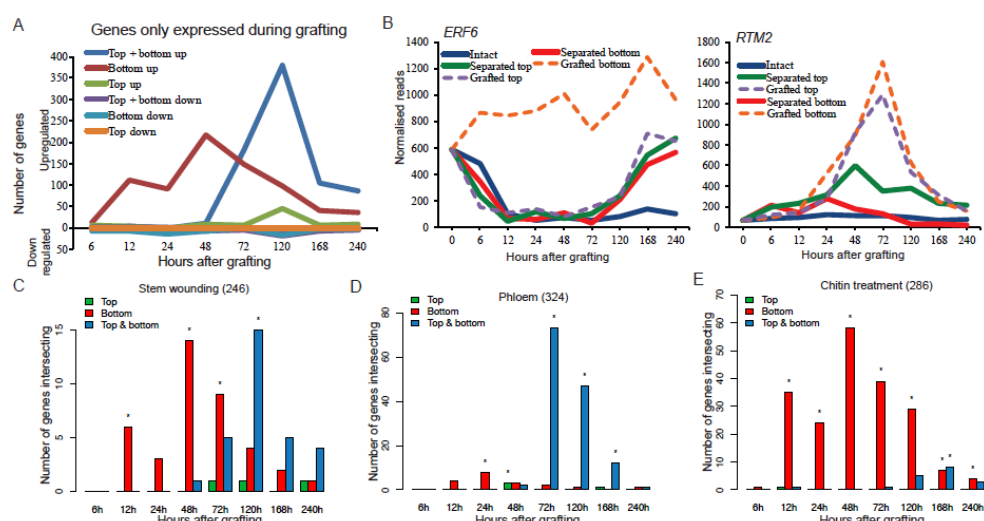
Figure 7. A subset of genes is differentially expressed only during graft formation when compared to 0 hour grafts, or intact or separated tissues. (A) Certain genes were only differentially expressed in grafted tops, grafted bottoms or both in grafted tops and grafted bottoms. (B) Expression profiles for a graft bottom-specific (*ERF6*) or a graft top and bottom differentially regulated gene (*RTM2*) were plotted for intact, separated and grafted samples. (C) Grafting-specific genes are also expressed in other processes of tissue fusion, such as stem healing. Here, 246 previously published RNAs whose differential expression is associated with stem healing were compared to our dataset to assess transcriptional overlap with the grafting-specific genes. Asterisks represent a significant high overlap ($p < 0.05$) of previously published genesets that are also differentially expressed in the grafted samples at a certain time point. (D-E) Genes differentially expressed in grafted tops and grafted bottoms show high overlap to 324 previously published genes whose transcripts are associated with phloem, whereas genes expressed in grafted bottoms show high overlap to 286 previously published genes whose encoded RNAs are associated with chitin treatment. Asterisks represent a significant high overlap ($p < 0.05$) of previously published genes that are also differentially expressed in the grafted samples at a certain time point.

DISCUSSION

To better understand how plants graft, we analysed in depth an RNA deep sequencing dataset that spatially and temporally distinguished genes activated by cutting followed by tissue attachment or continuous tissue separation. Cutting promoted a similar wound response in both grafted and separated tissues, however, by 72 hours after cutting the grafted and separated tissues became transcriptionally dissimilar (Figure 6C) indicating that tissue fusion was mechanistically different from healing an unattached cut surface. During graft formation, tissues had a very high transcriptional overlap with genes differentially expressed by inflorescence stem healing and by vascular induction in leaves (Figure 4, Figure S7) (9, 29) suggesting grafting is closely related to tissue reunion and vascular formation processes. Graft formation

474 had little transcriptional overlap with lateral root formation (Figure S6)(32) and

475 appeared to follow a pathway similar to secondary root growth (Figure S6, Figure S8)

476 since cambium markers *WOX4* and *PXY* that are specific to secondary growth were

477 expressed during grafting (38)(Figure S5). Grafted tops initially showed a short-

478 lasting and small transcriptional overlap with genes expressed during primary root

479 formation which may be related to the accumulation of substances activating

480 adventitious root formation, a common response in failed grafts or in cut shoots

481 (Figure S4C). Thus, we conclude that grafting proceeds via a pathway involving

482 secondary growth with radial meristems activating in the mature cambium to heal the

483 wound. Vascular formation genes including those specifying cambium and phloem

484 were activated early, followed by an activation of cell division genes, suggesting that

485 the start of cellular differentiation preceded activation of cell division. Xylem identity

486 genes showed an early and a late activation peak (Figure 3, Figure S5). There is no

487 visible xylem differentiation at the graft junction during the first peak of expression

488 (4) and these genes might be suppressed by phloem differentiation genes such as *APL*

489 and *CLE41* that activate early after grafting and are known to suppress protoxylem

490 formation (39, 40)(Figure S6)(Table S4). Alternatively, the first peak could represent

491 programmed-cell death that does not lead to xylem differentiation. The second

492 expression peak of xylem-expressed genes at 120 hours occurred after the

493 differentiation of functional phloem and coincided with the differentiation of xylem

494 strands at the graft junction (4). Previous studies highlighted the importance of callus

495 and pericycle cells during regeneration (16, 41), but we see little evidence that genes

496 expressed in the pericycle or during callus formation have high transcriptional overlap

497 with genes differentially expressed by grafting (Figure S4). Expression profiles for all

498 protein-coding genes can be found in table S4.

499

500 We observe only a slight delay in phloem, cambium and cell division activation

501 below the graft junction compared to above it (Figure 3, Figure S5, Figure S6)

502 whereas several genes associated with vascular formation, such as *HCA2* (42) and

503 *TMO6* (43)*,* activated equally in both grafted top and grafted bottom at 6 hours after

504 grafting (Figure 1D-G, Figure 3). These data indicate that, at least transcriptionally,

505 the grafted root rapidly responded to the presence of the grafted shoot and this

506 response was independent of functional vascular connections. This response was not

507 present in separated roots, indicating that attachment was key for recognition. Sugars

508   are known activators of cell division and cell elongation (13) and in our datasets, a

509   large proportion of asymmetrically expressed genes are genes that are sugar-

510   responsive. However, sugars are transported in the phloem (12) that is severed upon

511   grafting whereas the grafted root exhibited a sugar starvation response and showed

512   similar sugar-response dynamics as the separated root. Instead, we infer that not sugar

513   but auxin, or some other molecular that is transported in the absence of vascular

514   connections, could be the signal in the grafted bottom that activates *HCA2*, *TMO6* as

515   well as cell division, phloem- and cambium-related genes. Alternatively, separation

516   might cause a build-up of molecules from the root that suppress vascular induction

517   genes such as *HCA2* and *TMO6*.

518

519   Given auxin's role in vascular patterning and formation ((38), it is a strong candidate

520   for the activating signal. Auxin response was largely symmetric, particularly from 12

521   hours after grafting (Figure 6) consistent with previous findings that the auxin-

522   inducible *DR5* and *ANAC071* genes are symmetrically expressed around the graft

523   junction (4-6, 44). One idea is that auxin transport was not substantially interrupted by

524   the grafting process, and instead, where opposing tissues adhered, auxin moved

525   regardless of vascular connections since auxin is transported from cell to cell through

526   the apoplast (8). The genes encoding auxin efflux proteins PIN1 and ABCB1 were

527   transcriptionally activated above the graft junction (Figure 5D), similar to putative

528   *Pisum sativum* PIN1 protein accumulating above a cut stem prior to vascular

529   reconnection (45), and could reflect a role for these proteins in exporting auxin across

530   the cut. Consistent with these observations, adding an auxin transport inhibitor to

531   grafted *Arabidopsis* shoots prevented the expression of grafting-induced genes below

532   the graft junction (6). Since auxin is fundamental for patterning vasculature (38), it is

533   plausible that auxin movement across the graft occurs prior to sugar movement since

534   the flow of auxin could assist with reconnecting the phloem. Although auxin response

535   was symmetric, our previous work demonstrated that the auxin response factors *ALF4*

536   and *AXR1* affected grafting only below the graft junction (4). Mutating *ALF4* below

537   the graft junction more strongly reduced auxin response than mutating *ALF4* above

538   the junction (4). Thus, proteins such as ALF4 or AXR1 might enhance or promote

539   rootstock-specific auxin response and vascular regeneration that could be particularly

540   important when there is incomplete attachment, cellular damage or inefficient

541   transport. All higher plants transport auxin from shoot to root, yet not all plant species

542   can be successfully grafted (3) so the response to auxin rather than the transport itself

543   may be a determining factor in the ability to graft. A role for sugars is not completely

544   ruled out though, since the magnitude of differential expression was often lower in the

545   grafted bottom and exogenous sugar reduced grafting efficiency (Figure 2A).

546   Pericycle cells require auxin to divide and the addition of sugars enhances the rate of

547   divisions (46), suggesting that the presence of sugars in the grafted top enhanced cell

548   division and differentiation. Another hypothesis that warrants testing is whether graft

549   healing activates via a mechanical signal provided by the physical presence of the

550   opposing tissues.

551

552   Our analyses identified two groups of genes whose expression changes were unique

553   to graft formation in our experiments (Figure 7). One group activated shortly after

554   grafting below the graft junction and was enriched in immune-responsive and chitin-

555   responsive genes (Table S3, Figure 7, Figure S10). The breakdown products of cell

556   walls are potent elicitors of defence responses (47), so it is possible that the grafted

557   bottom upregulates pathways specific to wound damage response. This group was not

558   upregulated in separated bottoms though, so the unique physiological state of the

559   grafted root, indicated by the presence of auxin response but the absence of sugar

560   response, could have promoted their upregulation. The second group activated both

561   above and below the graft junction and became highly expressed later during graft

562   formation (Figure 7). This group was enriched in RNAs associated with vascular

563   development (Table S3, Figure 7) and we suggest that the products of these genes are

564   involved in the vascular reconnection processes between the two tissues. Despite

565   many transcriptional similarities between separated tops and grafted tissues, tissues

566   had to be attached for at least three days for phloem connections to form, regardless

567   of when cutting occurred (Figure S10). Thus, it appears that RNAs expressed in the

568   separated top or separated bottom are insufficient to drive graft formation. Instead

569   attachment and the genes activated by this recognition process including grafting-

570   specific RNA changes (Figure 7A) or RNAs expressed in the grafted bottom, grafted

571   top and separated top (Figure 6C) are those that contribute to a response that

572   distinguishes attached from separated plant tissues. Future work should focus on these

573   RNAs to identify the pathways required for grafting that could be modified to

574   improve graft formation, wound healing and vascular regeneration. Likewise, the

575   rapid transcriptional changes below the graft indicate a recognition system that

576 promotes tissue regeneration. Identifying the exogenous cue that triggers recognition

577 and understanding how it is perceived should be priorities, as should understanding

578 whether this phenomenon applies more broadly to inter-tissue communication, tissue

579 regeneration or tissue fusion events, such as parasitic plant infections (48), epidermal

580 fusions (49, 50) or petal fusions (51).

581

582 **METHODS**

583 **Plant material and microscopy**

584 *Arabidopsis thaliana* accession Columbia was used throughout. The *p35S::GFP-ER*

585 (52), *pSUC2::GFP* (53), *pUBQ10::PM-tdTomato* (54), *pARR5::GFP* (55),

586 *pANT::H2B-YFP* (56), *pLOG4::n3GFP* (57), *pCASP1::NLS-GFP* (58), *p35S::DII-*

587 *Venus* (35) lines have been previously published. For the construction of

588 *pHCA2::RFP*, a 2.9kb 5' upstream region of the *HCA2* gene was cloned into

589 pDONRp4-p1R donor vector, and recombined with tagRFPer into a destination vector

590 by the Multisite Gateway system (59). *Arabidopsis thaliana* micrografting and

591 grafting assays were performed according to previously published protocols (60, 61).

592 Fluorescent images were taken on a Zeiss LSM-700 or LSM-780 confocal

593 microscope. Black and white fluorescent images of graft junctions were taken on a

594 Zeiss V12 dissecting microscope. FIJI software (Fiji.sc) was used to process images.

595 A micro-extensometer was used for all breaking force graft measurements according

596 to a previously published protocol (62).

597

598 **RNAseq sample and library preparation**

599 Grafted wild type *Arabidopsis thaliana* accession Col-0 were harvested at the

600 respective time points and care taken to separate grafts by gently pulling plants apart.

601 Approximately 0.5mm of tissue was taken above or below each cut site and kept

602 separate. Intact plants had 1mm of tissue taken in a similar location on the hypocotyl

603 as separated or grafted plants. Grafted, separated or intact tissues were pooled into

604 groups of approximately 24 tissues . Tissues were ground using a microcentrifuge

605 pestle frozen in liquid nitrogen. RNA was extracted using an RNeasy Kit (Qiagen,

606 UK) following the manufacturer's instructions. 90-100ng of RNA was used to prepare

607 RNAseq libraries using the TruSeq® Stranded mRNA LT kit (Illumina, UK)

608 according to the manufacturer's instructions. The final PCR was for 15 cycles and 11-

609 12 barcoded samples were randomly mixed to make a total of 7 mixes for 7 flow

610 lanes, one mix per lane. Samples were sequenced on the HiSeq 4000 platform

611 (Illumina, UK) with Paired End 75bp transcriptome sequencing (BGI Tech Solutions,

612 Shenzhen, China).

613

614 **Iodine staining**

615 *Arabidopsis* seedlings were placed in a fixation solution (3.7% formaldehyde, 50%

616 ethanol, 5% acetic acid) for 1 hour at room temperature, then transferred to 70%

617 ethanol for 10 minutes. Afterwards, plants were transferred to 96% ethanol and stored

618 at -20°C for up to a week. Samples were rehydrated in 50% ethanol for 1 hour at

619 room temperature, transferred to distilled water for 30 minutes, then stained for 10

620 minutes in Lugol solution (Sigma) at room temperature. Plants were rinsed with water

621 and mounted on microscope slides. Images were taken on a Zeiss Axioimager.M2

622 microscope.

623

624 **Bioinformatic analyses**

625 The reads acquired through high-throughput sequencing were quality trimmed with

626 sickle (63) and aligned using the eXpress tool to protein-coding gene sequences

627 acquired from TAIR10 using Bowtie2. Library scaling factors were inferred from the

628 sum of the number of reads assigned to the genes in the lowest seventy-five

629 percentiles of expressed genes for each library (64). Analyses of the data were carried

630 out using the R package baySeq (36)and clustering based on the posterior

631 probabilities acquired from this package. The gene ontology analysis (GO)

632 enrichment analysis on grafting-specific genes was done with a customized R script

633 using the package GOstats (65).

634

642

643

REFERENCES

1. Goldschmidt EE (2014) Plant grafting: new mechanisms, evolutionary implications. *Front Plant Sci* 5:727.
2. Lee J, *et al.* (2010) Current status of vegetable grafting: Diffusion, grafting techniques, automation. *Sci Hortic-Amsterdam* 127:93-105.
3. Melnyk CW (2017) Plant grafting: insights into tissue regeneration. *Regeneration (Oxf)* 4(1):3-14.
4. Melnyk CW, Schuster C, Leyser O, & Meyerowitz EM (2015) A developmental framework for graft formation and vascular reconnection in Arabidopsis thaliana. *Curr Biol* 25(10):1306-1318.
5. Yin H, *et al.* (2012) Graft-union development: a delicate process that involves cell-cell communication between scion and stock for local auxin accumulation. *J Exp Bot* 63(11):4219-4232.
6. Matsuoka K, *et al.* (2016) Differential Cellular Control by Cotyledon-Derived Phytohormones Involved in Graft Reunion of Arabidopsis Hypocotyls. *Plant Cell Physiol* 57(12):2620-2631.
7. Matsumoto-Kitano M, *et al.* (2008) Cytokinins are central regulators of cambial activity. *P Natl Acad Sci USA* 105(50):20027-20031.
8. Leyser O (2011) Auxin, self-organisation, and the colonial nature of plants. *Curr Biol* 21(9):R331-337.
9. Asahina M, *et al.* (2011) Spatially selective hormonal control of RAP2.6L and ANAC071 transcription factors involved in tissue reunion in Arabidopsis. *P Natl Acad Sci USA* 108(38):16128-16132.
10. Wetmore RH & Rier JP (1963) Experimental induction of vascular tissues in callus of angiosperms. *Am J Bot* 50(5):418-430.
11. Aloni R (1980) Role of auxin and sucrose in the differentiation of sieve and tracheary elements in plant tissue cultures. *Planta* 150(3):255-263.
12. Lough TJ & Lucas WJ (2006) Integrative plant biology: Role of phloem long-distance macromolecular trafficking. *Annu Rev Plant Biol* 57:203-232.
13. Wang L & Ruan YL (2013) Regulation of cell division and expansion by sugar and auxin signaling. *Front Plant Sci* 4:163.
14. Chitwood DH, Guo M, Nogueira FT, & Timmermans MC (2007) Establishing leaf polarity: the role of small RNAs and positional signals in the shoot apex. *Development* 134(5):813-823.
15. Cheong YH, *et al.* (2002) Transcriptional profiling reveals novel interactions between wounding, pathogen, abiotic stress, and hormonal responses in Arabidopsis. *Plant Physiol* 129(2):661-677.
16. Iwase A, *et al.* (2011) The AP2/ERF transcription factor WIND1 controls cell dedifferentiation in Arabidopsis. *Curr Biol* 21(6):508-514.
17. Ikeuchi M, *et al.* (2017) Wounding triggers callus formation via dynamic hormonal and transcriptional changes. *Plant Physiol*.
18. Cookson SJ, *et al.* (2013) Graft union formation in grapevine induces transcriptional changes related to cell wall modification, wounding, hormone signalling, and secondary metabolism. *J Exp Bot* 64(10):2997-3008.
19. Cookson SJ, *et al.* (2014) Heterografting with nonself rootstocks induces genes involved in stress responses at the graft interface when compared with autografted controls. *J Exp Bot* 65(9):2473-2481.
20. Zheng BS, *et al.* (2010) cDNA-AFLP analysis of gene expression in hickory (Carya cathayensis) during graft process. *Tree Physiol* 30(2):297-303.

693   21.   Chen Z, *et al.* (2017) Transcriptome changes between compatible and
694   incompatible graft combination of Litchi chinensis by digital gene expression
695   profile. *Sci Rep* 7(1):3954.
696   22.   Lindsay DW, Yeoman MM, & Brown R (1974) An analysis of the
697   development of the graft union in Lycopersicon esculentum. *Ann Bot-London*
698   38:639-646.
699   23.   Moore R (1984) Graft formation in Solanum pennellii (Solanaceae). *Plant
700   Cell Rep* 3(5):172-175.
701   24.   Marsch-Martinez N, *et al.* (2013) An efficient flat-surface collar-free grafting
702   method for Arabidopsis thaliana seedlings. *Plant Methods* 9(1):14.
703   25.   Villadsen D & Smith SM (2004) Identification of more than 200 glucose-
704   responsive Arabidopsis genes none of which responds to 3-O-methylglucose
705   or 6-deoxyglucose. *Plant Mol Biol* 55(4):467-477.
706   26.   Thum KE, Shin MJ, Palenchar PM, Kouranov A, & Coruzzi GM (2004)
707   Genome-wide investigation of light and carbon signaling interactions in
708   Arabidopsis. *Genome Biol* 5(2):R10.
709   27.   Cordoba E, Aceves-Zamudio DL, Hernandez-Bernal AF, Ramos-Vega M, &
710   Leon P (2015) Sugar regulation of SUGAR TRANSPORTER PROTEIN 1
711   (STP1) expression in Arabidopsis thaliana. *J Exp Bot* 66(1):147-159.
712   28.   Osuna D, *et al.* (2007) Temporal responses of transcripts, enzyme activities
713   and metabolites after adding sucrose to carbon-deprived Arabidopsis
714   seedlings. *Plant J* 49(3):463-491.
715   29.   Kondo Y, *et al.* (2016) Vascular Cell Induction Culture System Using
716   Arabidopsis Leaves (VISUAL) Reveals the Sequential Differentiation of
717   Sieve Element-Like Cells. *Plant Cell* 28(6):1250-1262.
718   30.   Furuta KM, *et al.* (2014) Plant development. Arabidopsis NAC45/86 direct
719   sieve element morphogenesis culminating in enucleation. *Science*
720   345(6199):933-937.
721   31.   Czechowski T, Stitt M, Altmann T, Udvardi MK, & Scheible WR (2005)
722   Genome-wide identification and testing of superior reference genes for
723   transcript normalization in Arabidopsis. *Plant Physiol* 139(1):5-17.
724   32.   Brady SM, *et al.* (2007) A high-resolution root spatiotemporal map reveals
725   dominant expression patterns. *Science* 318(5851):801-806.
726   33.   Nemhauser JL, Hong F, & Chory J (2006) Different plant hormones regulate
727   similar processes through largely nonoverlapping transcriptional responses.
728   *Cell* 126(3):467-475.
729   34.   Abel S, Nguyen MD, & Theologis A (1995) The PS-IAA4/5-like family of
730   early auxin-inducible mRNAs in Arabidopsis thaliana. *J Mol Biol* 251(4):533-
731   549.
732   35.   Brunoud G, *et al.* (2012) A novel sensor to map auxin response and
733   distribution at high spatio-temporal resolution. *Nature* 482(7383):103-106.
734   36.   Hardcastle TJ & Kelly KA (2010) baySeq: empirical Bayesian methods for
735   identifying differential expression in sequence count data. *BMC
736   Bioinformatics* 11:422.
737   37.   Hardcastle TJ & Papatheodorou I (2017) clusterSeq: methods for identifying
738   co-expression in high-throughput sequencing data. *bioRxiv* 188581.
739   38.   De Rybel B, Mahonen AP, Helariutta Y, & Weijers D (2016) Plant vascular
740   development: from early specification to differentiation. *Nat Rev Mol Cell
741   Biol* 17(1):30-40.

742 39. Bonke M, Thitamadee S, Mahonen AP, Hauser MT, & Helariutta Y (2003)
743   APL regulates vascular tissue identity in Arabidopsis. *Nature* 426(6963):181-
744   186.
745 40. Ito Y*, et al.* (2006) Dodeca-CLE peptides as suppressors of plant stem cell
746   differentiation. *Science* 313(5788):842-845.
747 41. Sugimoto K, Jiao Y, & Meyerowitz EM (2010) Arabidopsis regeneration from
748   multiple tissues occurs via a root development pathway. *Dev Cell* 18(3):463-
749   471.
750 42. Guo Y, Qin G, Gu H, & Qu LJ (2009) Dof5.6/HCA2, a Dof transcription
751   factor gene, regulates interfascicular cambium formation and vascular tissue
752   development in Arabidopsis. *Plant Cell* 21(11):3518-3534.
753 43. Gardiner J, Sherr I, & Scarpella E (2010) Expression of DOF genes identifies
754   early stages of vascular development in Arabidopsis leaves. *Int J Dev Biol*
755   54(8-9):1389-1396.
756 44. Pitaksaringkarn W, Ishiguro S, Asahina M, & Satoh S (2014) ARF6 and
757   ARF8 contribute to tissue reunion in incised Arabidopsis inflorescence stems.
758   *Plant Biotechnol-Nar* 31(1):49-53.
759 45. Sauer M*, et al.* (2006) Canalization of auxin flow by Aux/IAA-ARF-
760   dependent feedback regulation of PIN polarity. *Genes Dev* 20(20):2902-2911.
761 46. Skylar A, Sung F, Hong F, Chory J, & Wu X (2011) Metabolic sugar signal
762   promotes Arabidopsis meristematic proliferation via G2. *Dev Biol* 351(1):82-
763   89.
764 47. Souza CA*, et al.* (2017) Cellulose-Derived Oligomers Act as Damage-
765   Associated Molecular Patterns and Trigger Defense-Like Responses. *Plant*
766   *Physiol* 173(4):2383-2398.
767 48. Musselman LJ (1980) The biology of Striga, Orobanche, and other root-
768   parasitic weeds. *Annual Review of Phytopathology* 18:463-489.
769 49. Lolle SJ, Hsu W, & Pruitt RE (1998) Genetic analysis of organ fusion in
770   Arabidopsis thaliana. *Genetics* 149(2):607-619.
771 50. Becraft PW, Stinard PS, & McCarty DR (1996) CRINKLY4: A TNFR-like
772   receptor kinase involved in maize epidermal differentiation. *Science*
773   273(5280):1406-1409.
774 51. Zhong J & Preston JC (2015) Bridging the gaps: evolution and development
775   of perianth fusion. *New Phytol* 208(2):330-335.
776 52. Nelson BK, Cai X, & Nebenfuhr A (2007) A multicolored set of in vivo
777   organelle markers for co-localization studies in Arabidopsis and other plants.
778   *The Plant journal* 51(6):1126-1136.
779 53. Imlau A, Truernit E, & Sauer N (1999) Cell-to-cell and long-distance
780   trafficking of the green fluorescent protein in the phloem and symplastic
781   unloading of the protein into sink tissues. *Plant Cell* 11(3):309-322.
782 54. Segonzac C*, et al.* (2012) The shoot apical meristem regulatory peptide CLV3
783   does not activate innate immunity. *Plant Cell* 24(8):3186-3192.
784 55. Yanai O*, et al.* (2005) Arabidopsis KNOXI proteins activate cytokinin
785   biosynthesis. *Curr Biol* 15(17):1566-1571.
786 56. Randall RS*, et al.* (2015) AINTEGUMENTA and the D-type cyclin CYCD3;1
787   regulate root secondary growth and respond to cytokinins. *Biol Open*.
788 57. De Rybel B*, et al.* (2014) Plant development. Integration of growth and
789   patterning during vascular tissue formation in Arabidopsis. *Science*
790   345(6197):1255215.

791   58. Roppolo D, *et al.* (2011) A novel protein family mediates Casparian strip
792   formation in the endodermis. *Nature* 473(7347):380-383.
793   59. Siligato R, *et al.* (2016) MultiSite Gateway-Compatible Cell Type-Specific
794   Gene-Inducible System for Plants. *Plant Physiol* 170(2):627-641.
795   60. Melnyk CW (2017) Grafting with Arabidopsis thaliana. *Methods Mol Biol*
796   1497:9-18.
797   61. Melnyk CW (2017) Monitoring Vascular Regeneration and Xylem
798   Connectivity in Arabidopsis thaliana. *Methods Mol Biol* 1544:91-102.
799   62. Robinson S, *et al.* (2017) An automated confocal micro-extensometer enables
800   in vivo quantification of mechanical properties with cellular resolution.
801   *bioRxiv* 183533.
802   63. Joshi NA & Fass JN (2011) Sickle: A sliding-window, adaptive, quality-based
803   trimming tool for FastQ files (Version 1.33)).
804   64. Hardcastle TJ, Kelly KA, & Baulcombe DC (2012) Identifying small
805   interfering RNA loci from high-throughput sequencing data. *Bioinformatics*
806   28(4):457-463.
807   65. Falcon S & Gentleman R (2007) Using GOstats to test gene lists for GO term
808   association. *Bioinformatics* 23(2):257-258.
809   66. Drost HG & Paszkowski J (2017) Biomartr: genomic data retrieval with R.
810   *Bioinformatics* 33(8):1216-1217.
811   67. Carlson M (2017) org.At.tair.db: Genome wide annotation for Arabidopsis), R
812   package version 3.4.1.

813
814
815
816
817
818
819
820
821
822
823
824
825
826
827
828
829
830
831

832 **SUPPORTING INFORMATION**

833 **SI Materials and Methods**

834

835 **Plant material and grafting**

836 *Arabidopsis thaliana* accession Columbia was used throughout. The *p35S::GFP-ER*

837 (52), *pSUC2::GFP* (53), *pUBQ10::PM-tdTomato* (54), *pARR5::GFP* (55),

838 *pANT::H2B-YFP* (56), *pLOG4::n3GFP* (57), *pCASP1::NLS-GFP* (58), *p35S::DII-*

839 *Venus* (35) lines have been previously published. For the construction of

840 *pHCA2::RFP*, a 2.9kb 5' upstream region of the *HCA2* gene was cloned into

841 pDONRp4-p1R donor vector, and recombined with tagRFPer into a destination vector

842 by the Multisite Gateway system (59). The following primers were used for *pHCA2*

843 cloning: attB4_HCA2(-)2958

844 GGGACAACTTTGTATAGAAAGTTGtcgatacgcgggacagatatac

845 attB1_HCA2ProEnd ggggACTGCTTTTTTGTACAAACTTGttttgtgttctgtatgtttg.

846 *Arabidopsis thaliana* micrografting was performed according to a previously

847 published protocol (60). Briefly, seven day old *Arabidopsis* seedlings were grown

848 vertically on Murashige and Skoog (MS) medium + 1% bacto agar (pH5.7; no

849 sucrose) in short day conditions (8 hours of 80-100 µmol m^{-2} s^{-1} light) at 20°C.

850 Seedlings were placed on one layer of 2.5x4cm sterile Hybond N membrane (GE

851 Healthcare) on top of two 8.5cm circles of sterile 3 Chr Whatman paper (Scientific

852 Laboratory Supplies) moisten with sterile distilled water in a 9cm petri dish. In a

853 laminar flow hood using a dissecting microscope, one cotyledon was removed and a

854 transvers cut through the hypocotyl was made with a vascular dissecting knife (Ultra

855 Fine Micro Knife; Fine Science Tools). Grafts were assembled by aligning the two

856 cut halves and joining them together, after which, the petri dishes was sealed with

857 parafilm and placed vertically under short day conditions at 20°C. For grafting on a

858 microscope coverslip to image the graft junction, a 10cm square Petri dish modified

859 by gluing a microscope coverslip in place of a section of plastic from the back. On top

860 of the microscope cover slip was placed a 2.5x4 cm rectangle of Hybond N

861 membrane. At the edges and base of the Petri dish three 3 x 8cm strips of Whatman

862 paper were placed. Sterile water moistened both Whatman paper and Hybond N.

863 After which, roots were placed on the Hybond N membrane and hypocotyls on the

864 coverslip. Grafting then proceeded as above. Graft junctions were imaged through the

865 coverslip with a Plan-Apochromat 20X/0.8 objective on a Zeiss LSM-700 or LSM-

866 780 confocal microscope.

867

Fluorescent assays and microscopy

869 To test the effect of sugars on grafting, *Arabidopsis thaliana* Col-0 plants were grown

870 on 1/2MS+ 1% bacto agar (pH5.7; no sucrose) for seven days in short day conditions.

871 Wild type roots were grafted to scions expressing *pSUC2::GFP* using the protocol

872 described above but either water or water containing 0.25%, 0.5% 1% or 2% sucrose

873 was added to the grafted plates. Roots were observed for fluorescence 2-7 days after

874 grafting with a Zeiss V12 dissecting microscope equipped with a GFP filter. Roots

875 were scored daily and the same plants were observed during the 7-day assay as

876 previously described (61).

877

878 Fluorescent images were taken on a Zeiss LSM-700 or LSM-780 confocal microscope

879 with a Zeiss Plan-Apochromat 20X/0.8 dry objective. A 488nm argon laser (Zeiss

880 780) or 488nm solid-state laser (Zeiss 700) was used for excitation of GFP and YFP.

881 A 561nm solid-state laser was used for excitation of the tdTomato fluorescent protein.

882 A T-PMT detector obtained bright-field transmitted light. Black and white fluorescent

883 images of graft junctions were taken on a Zeiss V12 dissecting microscope fitted with

884 a Hamamatsu EM-CCD camera and RFP and YFP filters. FIJI software (Fiji.sc) was

885 used to process images. Image contrast and brightness were adjusted for controls and

886 samples equally. For longitudinal images of the graft junction, z-stack projections are

887 shown and made with the average intensity function in FIJI from stacks containing the

888 hypocotyl vascular tissues, mesophyll and epidermis.

889

RNAseq sample and library preparation

891 Wild type *Arabidopsis thaliana* accession Col-0 were grafted as above taking care to

892 switch shoot and root between different plants. All grafting and cutting was

893 performed in the morning to minimize circadian effects. For the 0 hour time points,

894 plants were transferred from 1/2MS plates to the grafting plates and immediately

895 harvested. Only intact plants were harvested at the 0 hour time since at this point,

896 there would be insufficient time to reasonably expect the separated or grafted samples

897 to be transcriptionally different (the time between cutting and freezing is less than two

898 minutes). For all other time points, after cutting plants were left on grafting plates for

899   the respective amount of time. Tissues were harvested and care taken to separate

900   grafts by gently pulling plants apart. Approximately 0.5mm of tissue was taken above

901   or below each cut site and kept separate. Intact plants had 1mm of tissue taken in a

902   similar location on the hypocotyl as separated or grafted plants. Grafted, separated or

903   intact tissues were pooled into groups of approximately 24 tissues (1 plates with 24

904   plants) which were immediately placed in 96% ethanol on dry ice. After harvesting,

905   microcentrifuge tubes were briefly centrifuged and the ethanol removed before

906   storing at -80°C. Plants were grafted over two months to get sufficient material.

907

908   Tissues were ground in the microcentrifuge tube using a microcentrifuge pestle frozen

909   in liquid nitrogen. RNA was extracted using an RNeasy Kit (Qiagen, UK) following

910   the manufacturer's instructions including on column DNase digestion. RNA was

911   eluted from the column with 50ul of sterile water. Quality and quantity of RNA was

912   checked using an Agilent 2200 TapeStation and High Sensitivity (HS) RNA

913   screentapes (Agilent, UK). After RNA extraction, two to four biological replicates

914   were combined (50-100 plants) to get sufficient RNA. 90-100ng of RNA was used to

915   prepare RNAseq libraries using the TruSeq® Stranded mRNA LT kit (Illumina, UK)

916   according to the manufacturer's instructions. The final PCR was for 15 cycles and

917   samples were resuspended in 23ul of distilled water. Quantity and quality of DNA

918   libraries was checked on the Agilent 2200 TapeStation using D1000 screentapes

919   (Agilent, UK). Each sample had two libraries prepared from grafted tissues or

920   separated tissues at different times so that independent biological replicates were

921   made. Samples were diluted to 10nM and 11-12 barcoded samples randomly mixed to

922   make a total of 7 mixes for 7 flow lanes, one mix per lane. Samples were sequenced

923   on the HiSeq 4000 platform (Illumina, UK) with Paired End 75bp transcriptome

924   sequencing (BGI Tech Solutions, Shenzhen, China).

925

926   **Iodine staining**

927   *Arabidopsis* seedlings were placed in a fixation solution (3.7% formaldehyde, 50%

928   ethanol, 5% acetic acid) for 1 hour at room temperature, then transferred to 70%

929   ethanol for 10 minutes. Afterwards, plants were transferred to 96% ethanol and stored

930   at -20°C for up to a week. Samples were rehydrated in 50% ethanol for 1 hour at

931   room temperature, then transferred to distilled water for 30 minutes. Samples were

932   then transferred to a solution of Lugol solution (Sigma) and stained for 10 minutes at

933　　room temperature. Plants were rinsed with water, then mounted on microscope slides.

934　　Images were taken on a Zeiss Axioimager.M2 microscope with a PlanApochromat

935　　20x objective and SPOT Flex camera (Imsol, UK).

936

937　　**Pairwise and Bayseq analyses**

938　　The reads acquired through high-throughput sequencing were quality trimmed with

939　　sickle (63) to increase the read quality before mapping. Reads were aligned to

940　　protein-coding gene sequences acquired from TAIR10 using Bowtie2. Read

941　　assignment was performed using the eXpress tool, which also provided effective gene

942　　lengths for use in normalisation. Library scaling factors were inferred from the sum of

943　　the number of reads assigned to the genes in the lowest seventy-five percentiles of

944　　expressed genes for each library (64).

945

946　　Analyses of the data were carried out using the R package baySeq (36)and clustering

947　　based on the posterior probabilities acquired from this package. For each timepoint,

948　　all possible patterns of differential expression between the graft types were

949　　considered, where a 'pattern' defines similarity and difference between different

950　　experimental conditions. For example,

951　　*'{Col_cut_bottomGenes=Col:Col_bottomGenes=ungraftedGenes},{Col_cut_topGenes=Col:Col_topGenes}'*

952　　defines a pattern in which gene expression is equivalent in the separated bottoms, the

953　　grafted bottoms and the intact plant, but different to the equivalently expressed

954　　separated top and grafted top. The total number of possible patterns for five

955　　experimental conditions (as in this analysis) is fifty-two.

956

957　　For a given timepoint, posterior likelihoods on the likelihood of each pattern of

958　　expression are calculated for every gene with greater than ten reads across all

959　　experimental conditions. The patterns were then modified to include orderings

960　　(denoted by < or >), for example, the pattern described would lead to the ordered

961　　pattern

962　　*'{Col_cut_bottomGenes=Col:Col_bottomGenes=ungraftedGenes}>{Col_cut_topGenes=Col:Col_topGenes}'*

963　　in which gene expression is equivalent in the separated bottoms, the grafted bottoms

964　　and the intact plant and greater than the equivalently expressed separated top and

965　　grafted top. In total, 541 ordered patterns exist in this data set. Posterior likelihoods

966　　for an ordered pattern were assigned to that of the unordered pattern for genes in

967   which the (normalised) mean expressions within the equivalently expressed groups

968   conformed to the ordering, and to zero otherwise.

969

970   Based on the posterior likelihoods for the ordered patterns, a similarity score s_{ij} was

971   established between two genes i and j as the sum over the products of their likelihoods

972   of each ordered pattern. A single-link agglomerative clustering of genes, in which a

973   gene will join a cluster if it has a greater than 50% similarity to any gene within that

974   cluster was then performed based on these similarity scores. We label each cluster

975   according to the predominant ordered pattern with high likelihood amongst the genes

976   that comprise it. The change in size of these clusters over time is shown for the major

977   clusterings in Figure 6.

978

979   We can also find likelihoods on comparisons between pairs of experimental

980   conditions by summing the likelihoods over combinations of patterns. Figure 1B

981   shows the number of genes identified at each time point in a pairwise analysis

982   between the grafted top and grafted bottom samples. The likelihood of symmetric

983   expression (i.e., expression which is equivalent across the graft junction) is calculated

984   as the sum of the likelihoods of all patterns in which the grafted top and grafted

985   bottom samples are equivalent. Conversely, asymmetric expression is calculated as

986   the sum of the likelihoods of all patterns in which the grafted top and grafted bottom

987   samples are not equivalent. Additional sets can be formed by considering the ordering

988   of the grafted top and grafted bottoms samples. Sets of genes are identified at each

989   time point with an FDR of less than 0.05 and a likelihood of symmetric/asymmetric

990   expression greater than 50%. Genes in this analysis were only included if they were

991   differentially expressed relative to intact samples.

992

993   Gene overlap analyses of up and down regulated genes

994   To measure if the ratio of up- and down- regulated genes from a previously published

995   dataset is significantly different to the ratio of up- and down-regulated genes in our

996   grafting dataset we only took into account genes that are differentially expressed at a

997   certain time point. A gene was called differentially expressed at a certain time point if

998   the marginal likelihood, calculated by BaySeq, was greater than 0.9 and if the

999   absolute $\log_2$-foldchange was greater than 1. Hence, we only consider genes that are

1000   significantly two-fold up- or down- regulated. This definition of differentially

1001   expressed genes was also used to filter the published datasets according to the

1002   expression values in our transcriptome dataset. Hence, some genes were filtered out

1003   from the original published datasets because they did not show a significant up- or

1004   down- regulation during a certain time point in our expression data based on our

1005   criteria. The histograms (Figure 2,4, 5, S4, S7, S8, S9) show the relative number of

1006   up- and down- regulated genes from the published datasets during a certain time point

1007   and a certain condition (separated top, separated bottom, grafted top, grafted bottom)

1008   based on the number of genes in the published dataset after filtering. To calculate the

1009   significance of the difference of the ratios between the published DEGs and all up-

1010   and down- regulated genes, we used a two-sided Fisher's exact test. To correct for

1011   multiple testing we used the Benjamini-Yekutieli (BY) correction method. Hence, the

1012   asterisks in the barplots highlight that the corrected p-value is below 0.05.

1013

1014   **Dealing with probe ids from microarray datasets**

1015   Due to the fact that some published datasets only used probe ids instead of gene ids to

1016   represent their differentially expressed genes we first had to match these probe ids to

1017   their corresponding gene ids. This step was done with the R package biomartr (66). If

1018   one probe id matched more than one gene id we used all the corresponding gene ids

1019   and tested afterwards if these genes were actually differentially expressed in our

1020   dataset. In some cases, one probe id was represented by more than one gene id.

1021   Hence, some gene sets contained slightly more gene ids than published probe ids. In

1022   contrast, some probe ids did not match to currently existing gene ids. Hence, some

1023   gene sets contained slightly fewer gene ids than published probe ids.

1024

1025   **Gene overlap analyses of gene sets involved in graft formation**

1026   For this analysis we used the previously calculated gene sets from baySeq of

1027   differentially expressed genes clustered for each time point into grafted bottom,

1028   grafted top, and grafted bottom and top and calculated their overlap to previously

1029   published data sets. The significance of the number of overlapping genes between the

1030   grafted samples and the published datasets was determined by a one-sided Fisher's

1031   exact test, to prove if the overlap is greater than expected. The resulting p-values were

1032   corrected for multiple testing by using the Benjamini-Yekutieli method.

1033   This procedure was also applied to generate Table 1 to study the overlaps of

1034   symmetrically and asymmetrically expressed genes in the grafting dataset with

1035   previously published sugar-responsive genes.

1036

1037   **GO enrichment analysis**

1038   The gene ontology analysis (GO) enrichment analysis on grafting-specific genes was

1039   done with a customized R script using the package GOstats (65). Gene ontology

1040   annotation was used from the Bioconductor package org.At.tair.db (67). The p-values

1041   calculated by a hypergeometric test were corrected for multiple testing with the

1042   Bonferroni correction. A GO category was called enriched if the corrected p-value

1043   was below 0.05.

1044

1045   A detailed description, the required data and R scripts to reproduce the clustering

1046   (hierarchical clustering and PCA), the statistical analyses regarding the overlap

1047   studies, and the GO enrichment analysis are available via the GitHub repository

1048   (https://github.com/AlexGa/GraftingScripts).

1049

1050   **Breaking force measurements**

1051   A micro-extensometer was used for all breaking force graft measurements according

1052   to a previously published protocol (62). Briefly, grafted Col-0 plants were attached to

1053   a moving plate using tough tags (0.94X0.50 inches, white, 679 catalog no. TTSW-

1054   1000, DiversifiedBiotech) and a cyanoacrylate glue. The plates were moved apart and

1055   the force was measured using a force sensor (Futek LSB200 10g load cell, Futek

1056   Inc.). Upon breaking the force dropped. The maximum force measured before

1057   breaking was recorded. Images were captured using a Leica SP5 confocal microscope.

1058   During the experiment single z-place images were captured and made into a movie in

1059   ImageJ.

1060

1061   To measure levels of tissue contamination between grafted top and bottom, grafted

1062   green fluorescent protein(*p35S::GFP*) and red fluorescent protein (*pUBQ10::PM-*

1063   *tdTomato*) expressing plants were pulled apart manually and imaged on a Zeiss LSM

1064   700 confocal microscope. Z-stacks comprising the majority of the hypocotyl were

1065   made and regions approximately 0.5mm above and 0.5mm below the graft junction

1066   were made into projections using the average intensity function on FIJI software, and

1067   then the mean intensity quantified for red and green channels on FIJI. The mean

1068   intensity of one colour in the tissue tested for contamination was divided by the mean

1069   intensity of the same colour in the tissue expressing that transgenes to get a

1070   percentage of contamination. A region away from the cut site was also quantified to

1071   get a percentage of spectral overlap between red and green channels. The percent

1072   spectral overlap was then subtracted from the percentage contamination to get an

1073   overall percentage for how much contamination was present.

1074

1075

1076

1077

1078

1079

1080

1081

1082

1083

1084

1085

1086

1087

1088

1089

1090

1091

1092

1093

1094

1095

1096

1097

1098

1099

1100

Movie S1. Breaking weight measurements at the graft junction, related to figure 1. A micro-extensometer pulled apart an Arabidopsis plant 9 days after grafting while force was measured using a force sensor and images captured using a Zeiss Sp5 confocal microscope. Here, the transmitted light field is shown. Shoot is on top and root towards the bottom.

Movie S2. Breaking weight measurements at the graft junction, related to figure 1. A micro-extensometer pulled apart an *Arabidopsis* plant 9 days after grafting while force was measured using a force sensor and images captured using a Zeiss Sp5 confocal microscope. The same experiment is shown in Movie S1, but here, the GFP and RFP channels are shown. Shoot is on top (*p35S::GFP* expressing) and root towards the bottom (*pUBQ10::PM-tdTomato* expressing).

Table S1. Details of previously published datasets used to compare to the grafting datasets.

Table S2. Numbers and categories associated with the Bayseq analysis. Categories are defined as grafted (Col:Col), separated (Col_cut) or intact (ungrafted).

Table S3. GO analysis for biological process (BP). Shown are the top 20 BP GO terms for the grafting-specific genes. Time point selected are those when there are the most genes in grafted bottom samples (48hrs) or grafted top + bottom samples (120 hrs).

Table S4. Normalised reads for all the protein-coding genes in the datasets. By entering the ATG number of interest, a plot is made which shows a differential gene expression profile for the gene of interest.

Dataset S1. Details of the Bayesian segmentation analysis providing files containing the ATGs for every cluster for every time point.
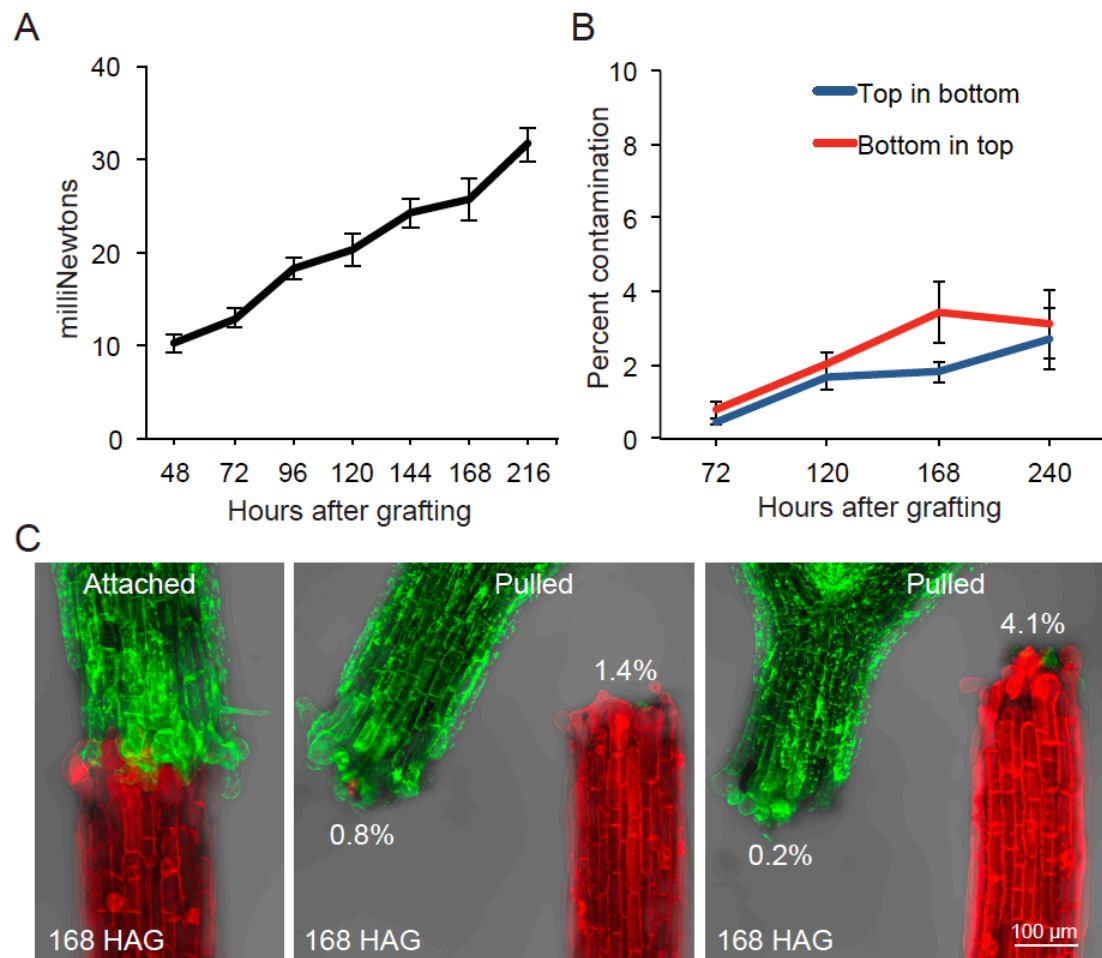
Figure S1. Experimental approach, related to figure 1. (A) The breaking weight required to pull apart grafted plants measured by a micro-extensometer. (B-C) Contamination of top in bottom or bottom in top was less than 4% as measured by grafting green fluorescent protein-expressing plants (*p35S::GFP*) to tomato fluorescent protein-expressing plants (*pUBQ10::PM-tdTomato*) and measuring amounts of fluorescence at the different wavelengths of emission in the top segments relative to the bottom. Images show different plants prior to and after pulling with the percent contamination indicated.

1142
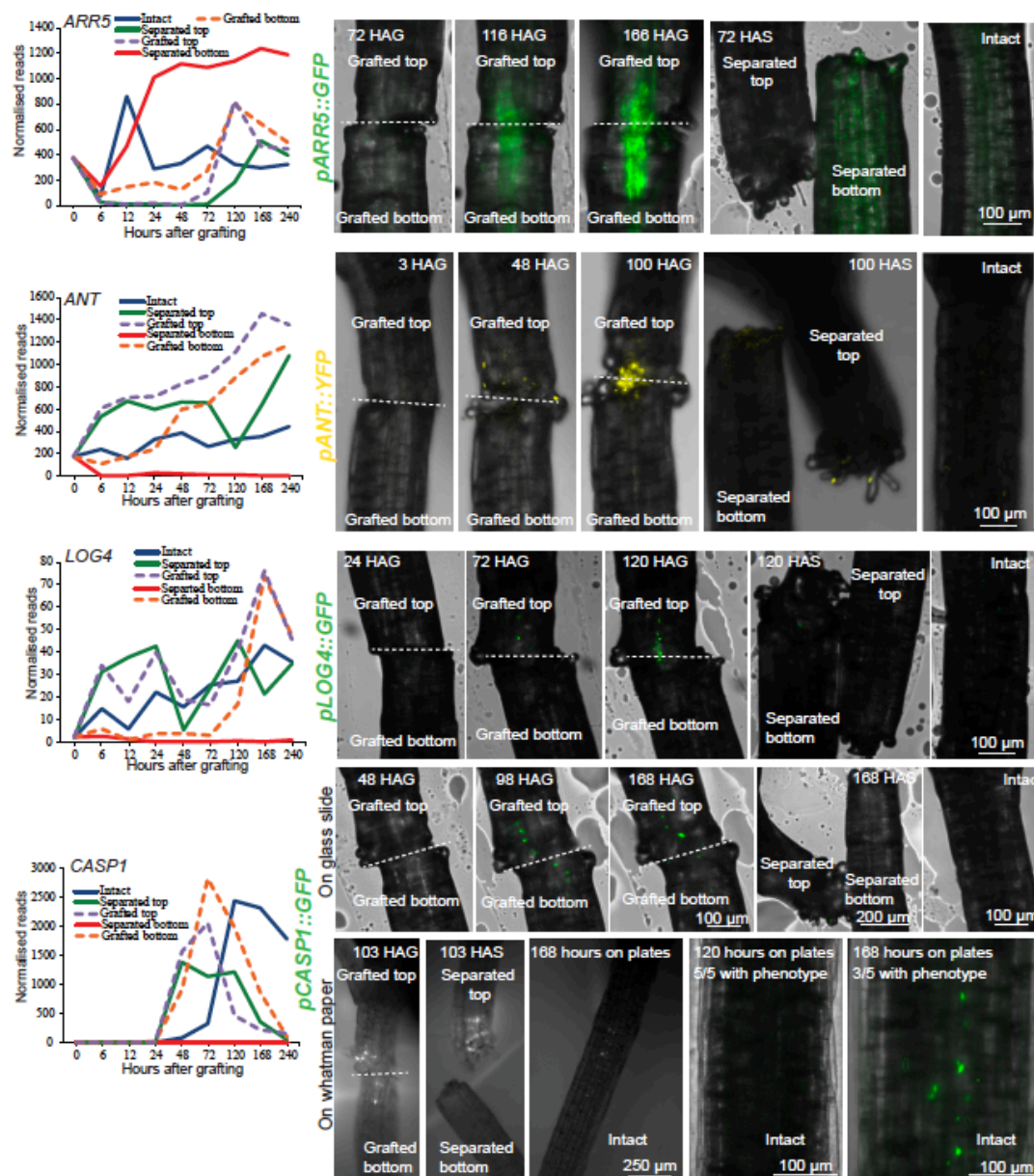
Figure S2. Comparison between RNAseq transcriptome expression profiles and transcriptional fluorescent reporters, related to figure 1. RNAseq expression profiles for various genes upregulated during graft formation were plotted for intact, separated and grafted samples (left panels). Transcriptional reporter-expressing plants were cut and separated, cut and grafted, or left intact. After cutting, plants were imaged and z-projections made at various time points (right panels). For *pCASP1::GFP*, we did not observe a signal in intact plants grafted on glass slides (see Materials and Methods), but observed a signal with 3/5 plants 7 days after grafting on Whatman-nylon membrane, the same condition used for transcriptome library preparation. HAG, hours after grafting. HAS, hours after separation. Dashed lines denote the graft junction.

1154

1155
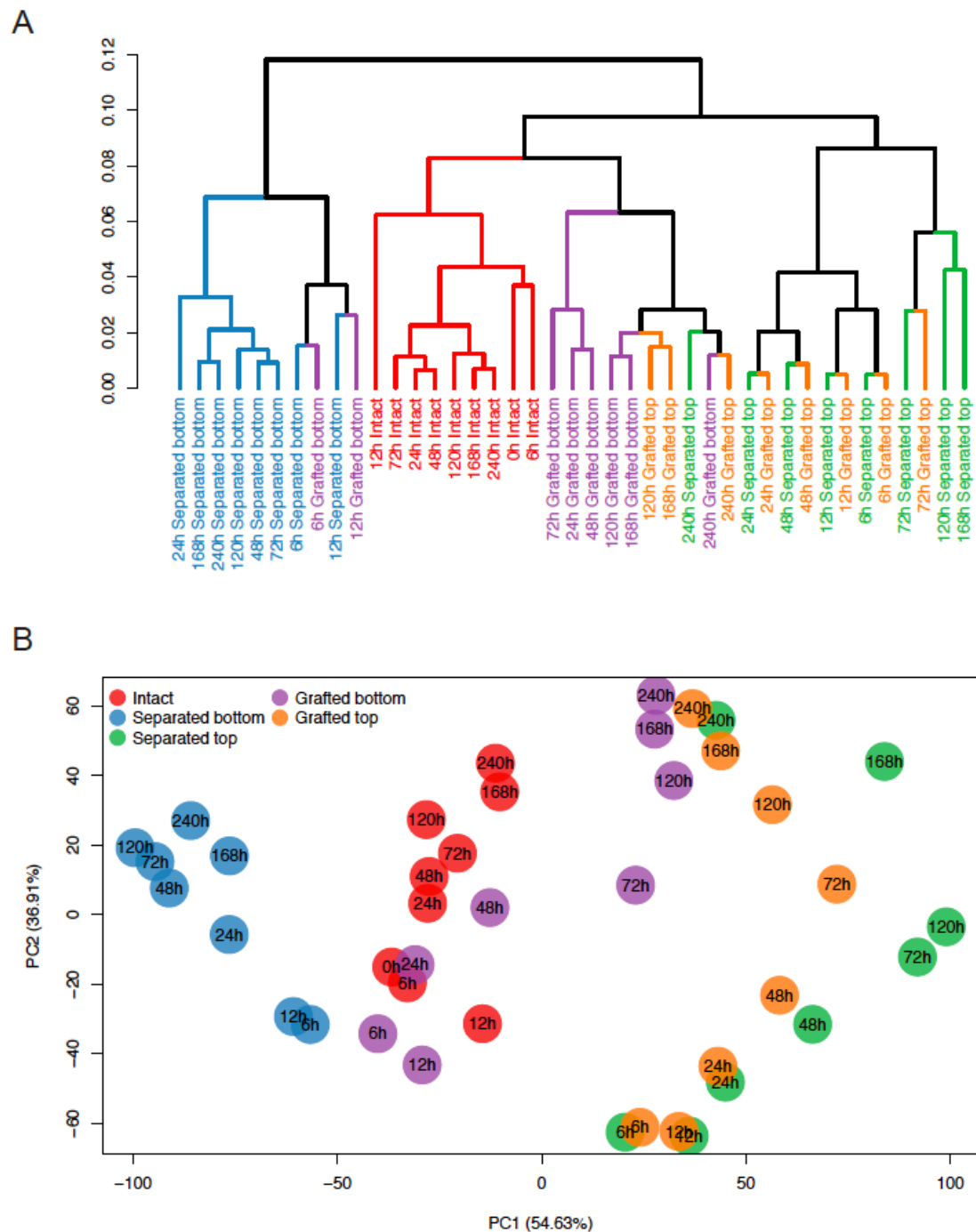
Figure S3. Hierarchical cluster analysis and principle component analysis (PCA) for the transcriptome libraries, related to figure 1. (A) Hierarchical clustering of samples based on log10 transformed TPM values. Similarity between samples was measured by 1 – spearman correlation coefficient. (B) PCA of expression data shows clustering of similar samples. Especially the grafted top and grafted bottom samples are very similar from 120 hours onwards.
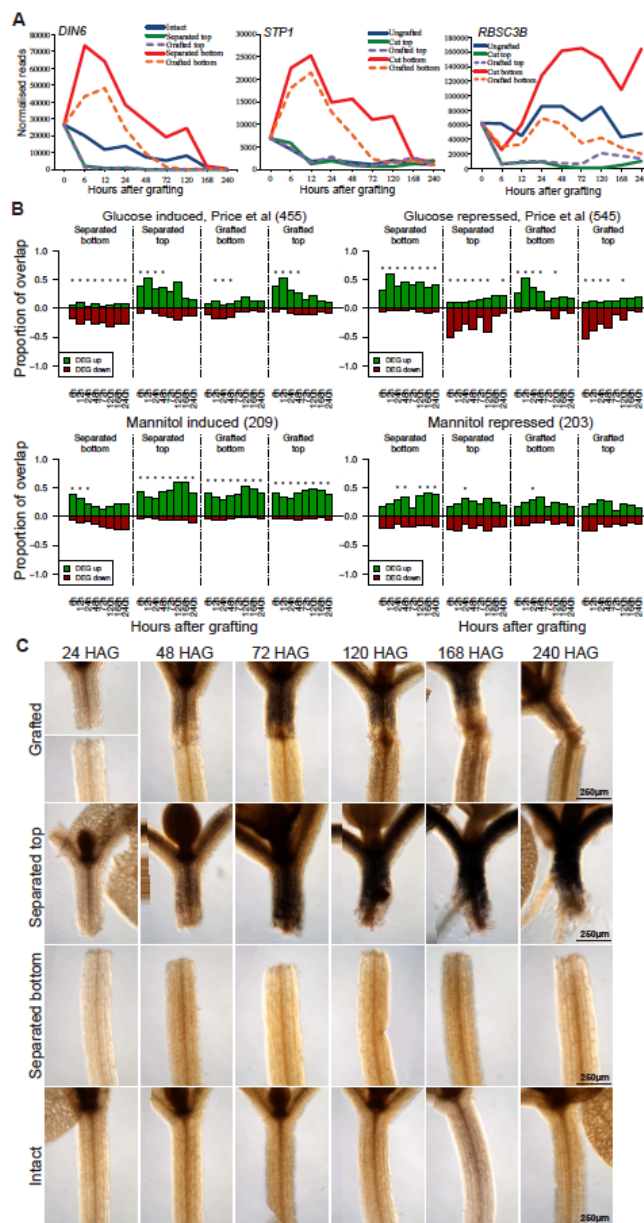
Figure S4. Asymmetry is a feature observed with sugar response and starch accumulation, related to figure 2. (A) Expression profiles for RNAs coded by sugar-repressed genes (*DIN6*, *STP1*) or photosynthetic gene (*RBSC3B*) were plotted for intact, separated and grafted samples. (B) Transcriptional overlap between previously published mannitol-induced, mannitol-repressed, sugar-induced or sugar-repressed genes and our datasets. The numbers in brackets represents the number of glucose or mannitol-responsive genes identified in the previous dataset, and overlap is presented as a ratio out of 1.0 for differentially expressed genes (DEG) up or down regulated in our dataset relative to intact samples. Asterisks represent a significant difference ($p < 0.05$) between the ratio of up- and down- regulated genes in a previously published transcriptome dataset compared to the ratio of all up- and down-regulated genes in our grafting dataset at a certain time point. (C) Lugol staining of grafted plants at various time points reveals dark brown staining associated with starch accumulation. Upper grafted panels are the same as those present in Figure 2 and shown here to compare with controls. HAG, hours after grafting.

1179
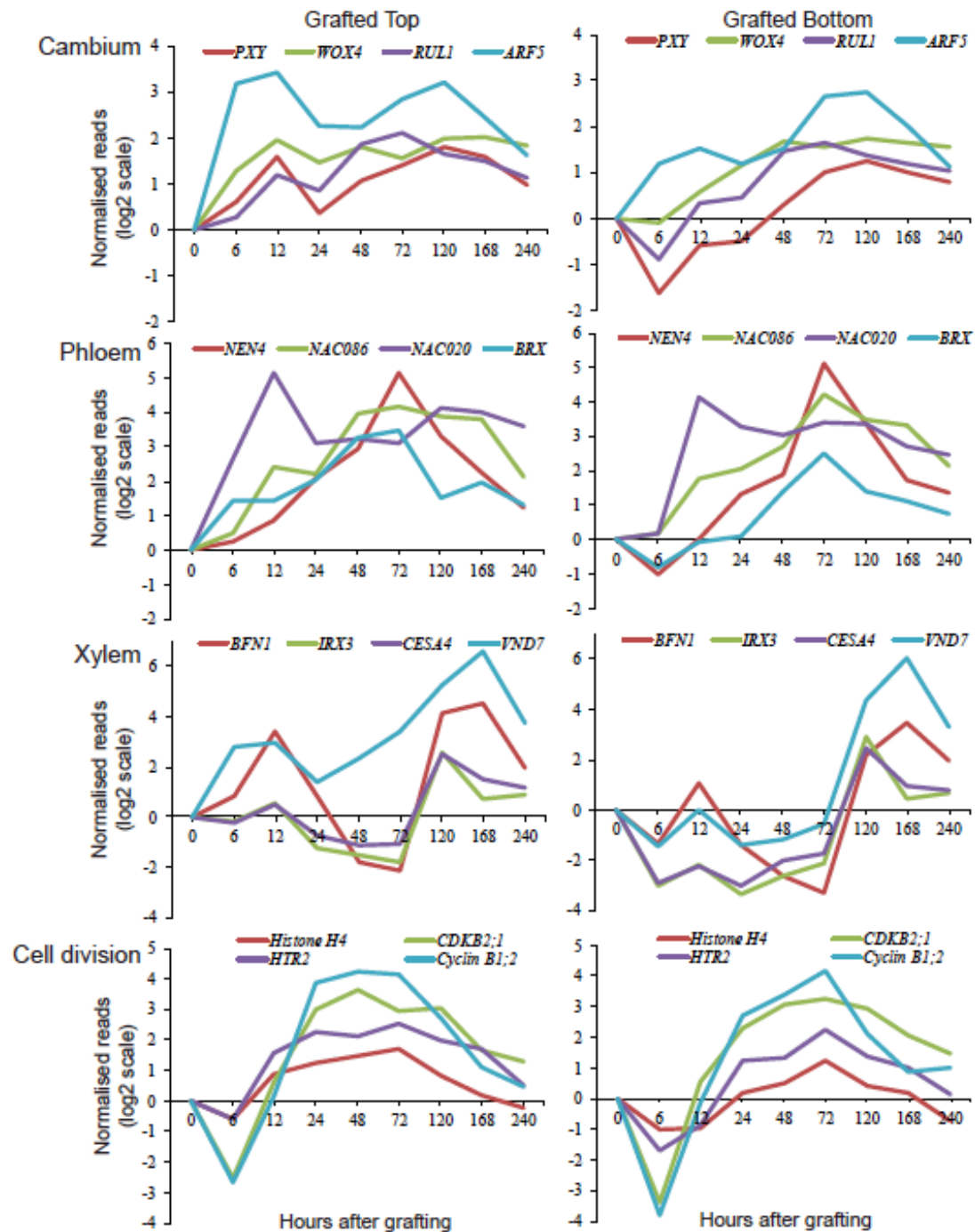
Figure S5. Transcriptional dynamics of genes associated with cambium, phloem, xylem and cell division, related to figure 3. Expression profiles in grafted tops or grafted bottoms for various genes of interest were plotted, normalised to intact samples and plotted on a $\log_2$ scale.
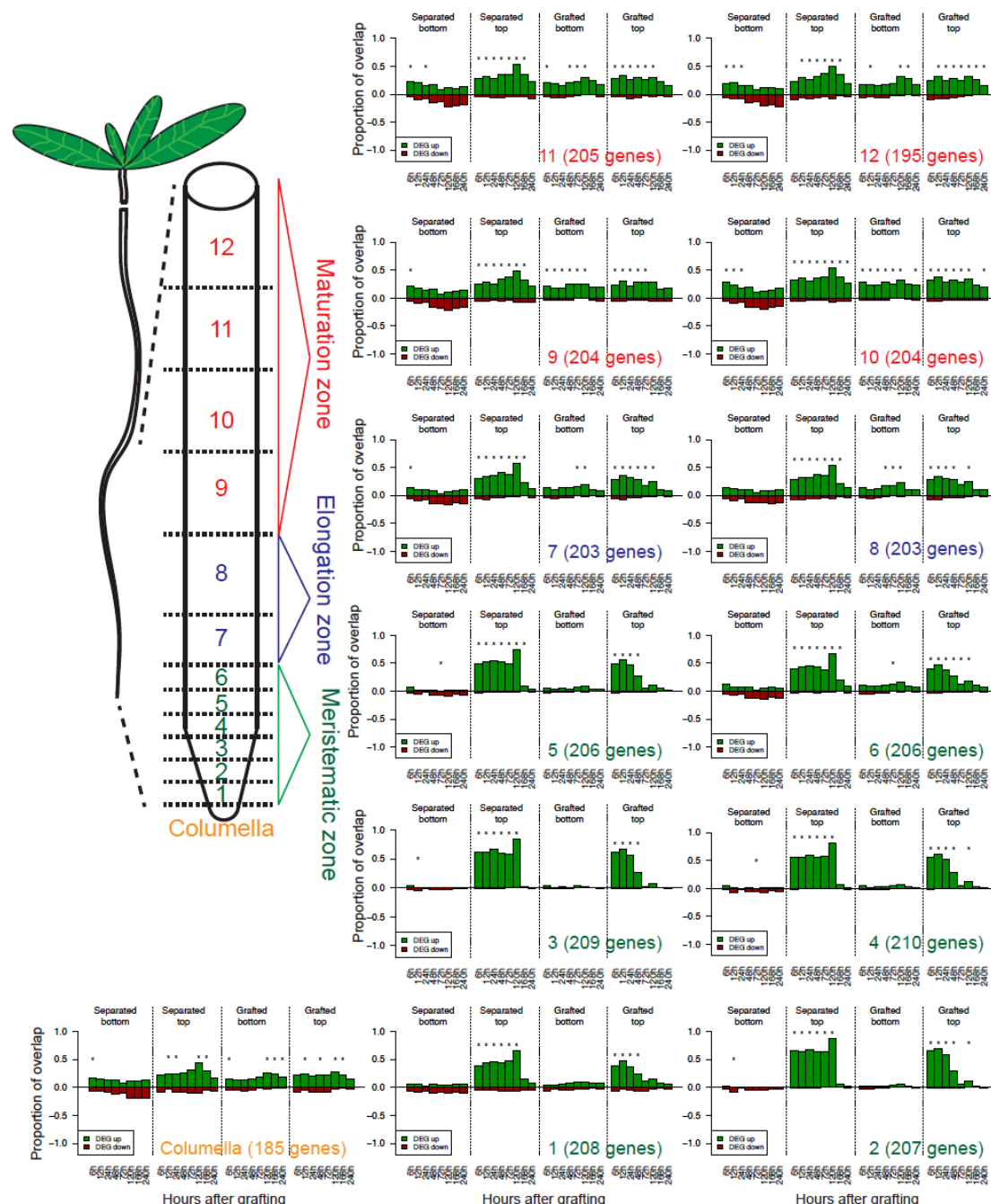
1180
1181
1182
1183
1184

1185
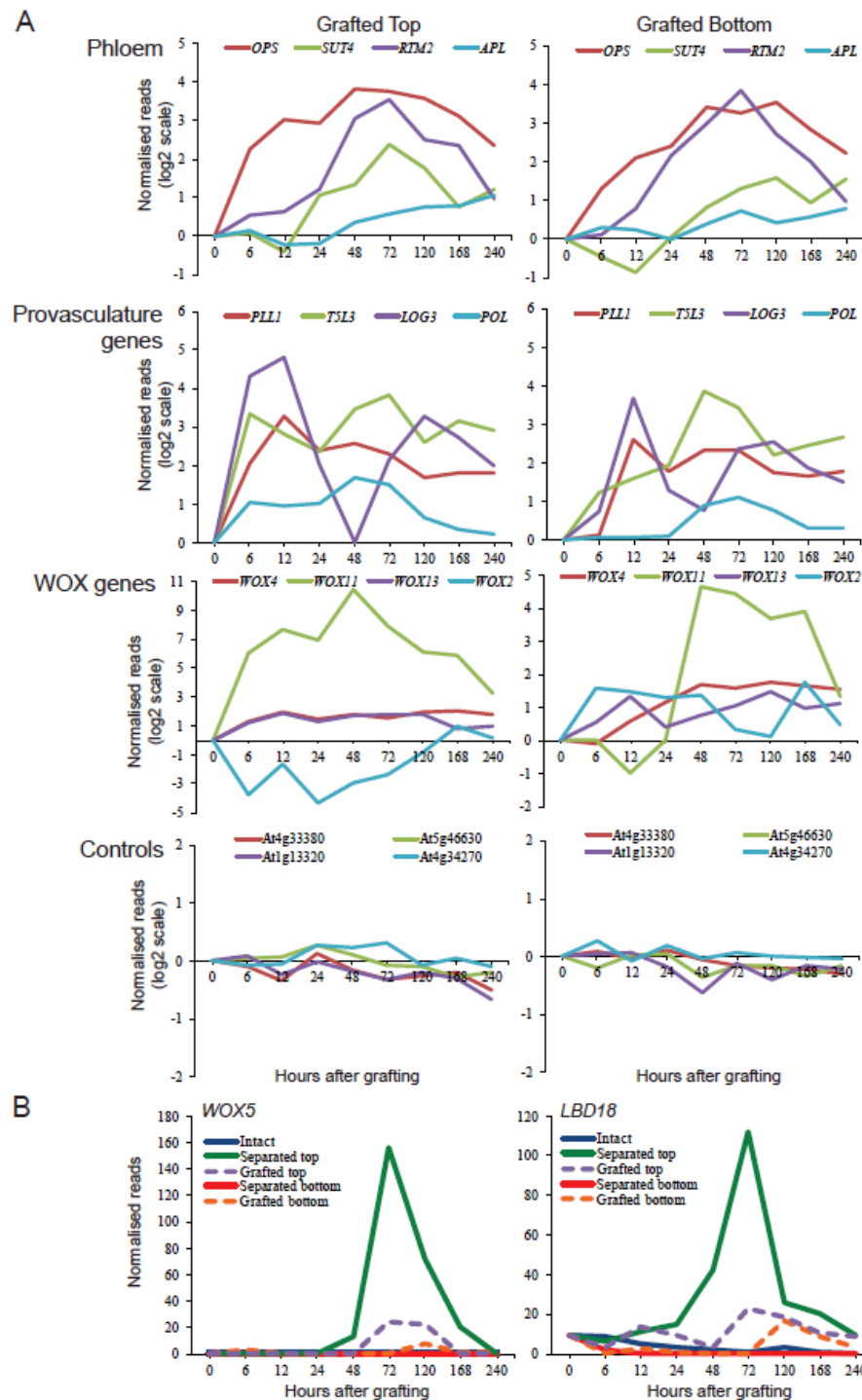
Figure S6. Accumulation of RNA from genes associated with provasculature and phloem, and of RNAs from WOX transcription factors, related to figure 3. (A) RNA accumulation profiles for various genes of interest were plotted over time as measured in grafted tops or grafted bottoms, normalised to intact samples and plotted on a $\log_2$ scale. The grafting datasets could also be used to investigate the transcriptional dynamics of related genes, such as the sequential activation of WOX transcription factors at the graft junction. (B) Expression levels of a primary root specific transcript (of the *WOX5* gene) or a lateral root specific transcript (from the *LBD18* gene) were plotted over time for intact, separated and grafted samples.
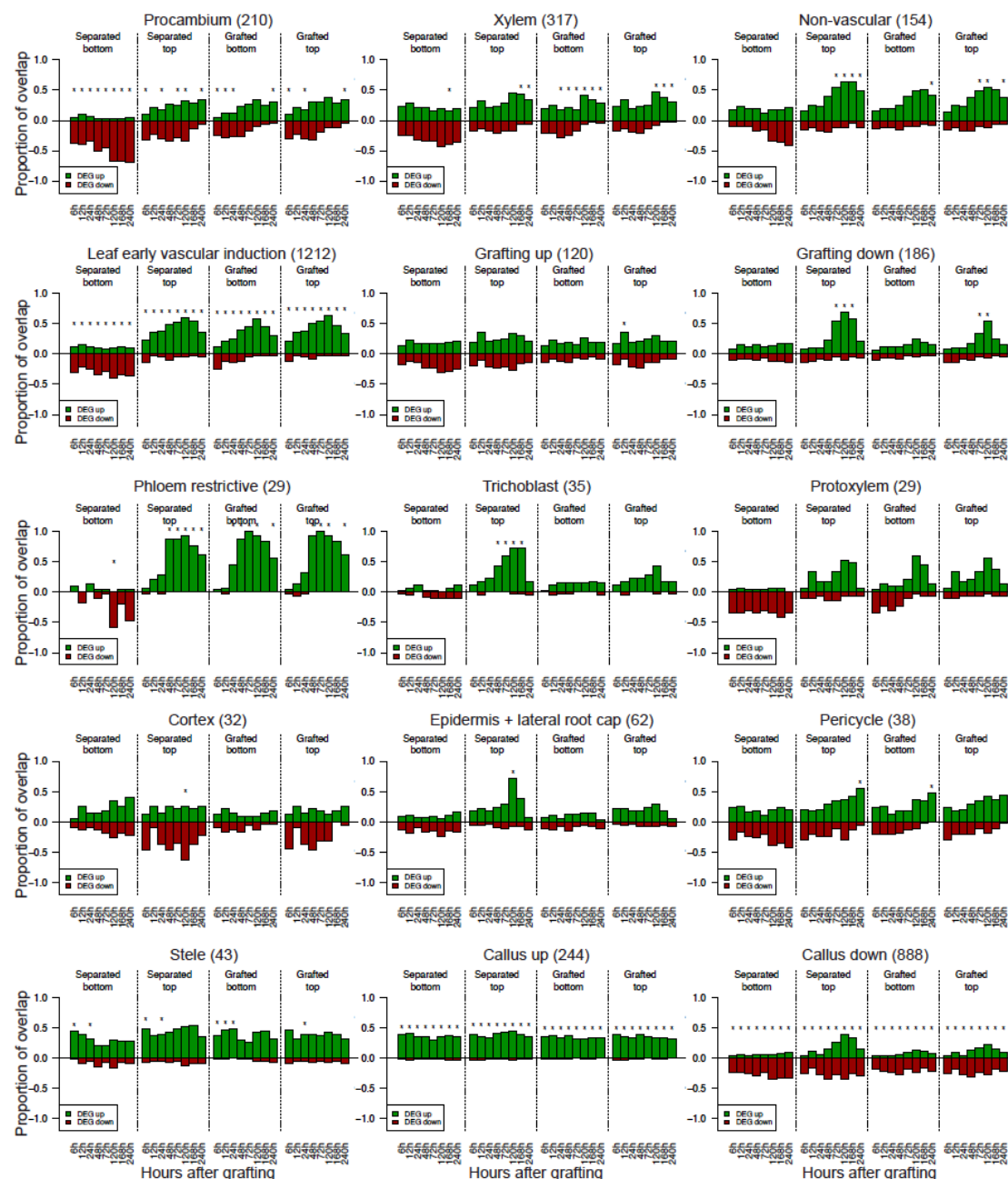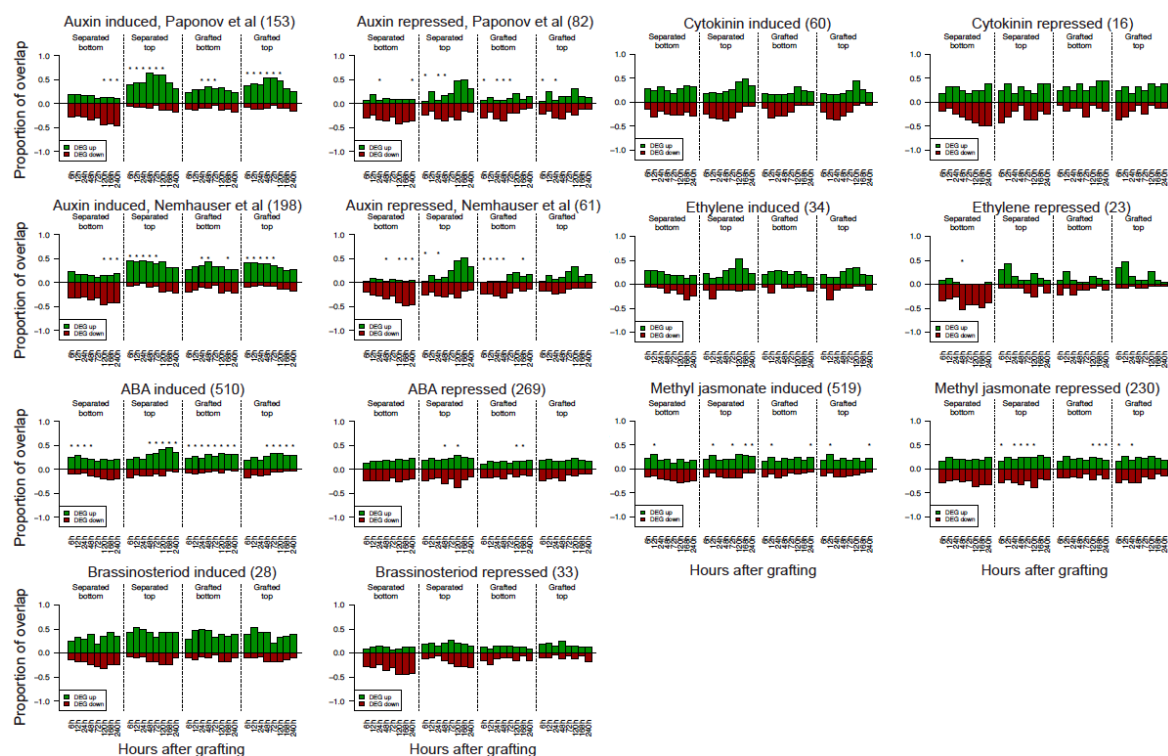
Figure S7. Transcriptional overlap between previously published datasets and the grafting datasets, related to Figure 4. Genes whose transcripts are associated with various cell types or biological processes were taken from previously published datasets (see Table S1) and compared to the datasets generated here. The number in brackets represents the number of cell type-specific or process-specific genes identified in the previous dataset, and overlap is presented as a ratio out of 1.0 for differentiation expressed genes (DEG) up- or down-regulated in our dataset relative to intact samples. Asterisks represent a significant difference ($p < 0.05$) between the ratio of up- and down- regulated genes in a previously published transcriptome dataset compared to the ratio of all up- and down- regulated genes in our grafting dataset at a certain time point.

Figure S8. Transcriptional overlap between previously published root transcriptomic datasets and the grafting RNA-seq dataset, related to Figure 4. Genes whose transcripts are associated with various root regions were taken from previously published datasets (see Table S1) and compared to the datasets generated here. Root layer is indicated in the bottom right of each histogram with reference to the cartoon. The number in brackets represents the number of root layer-specific genes identified in the previous dataset, and overlap is presented as a ratio out of 1.0 for differentiation expressed genes (DEG) up- or down-regulated in our dataset relative to intact samples. Asterisks represent a significant difference ($p < 0.05$) between the ratio of up- and down- regulated genes in a previously published transcriptome dataset compared to the ratio of all up- and down- regulated genes in our grafting dataset at a certain time point.

1223

1224

Figure S9. Transcriptional overlap between previously published hormone responsive RNA datasets and the grafting RNA datasets, related to Figure 5. Genes whose differential expression is associated with various hormone responses were taken from previously published datasets (see Table S1) and compared to the genes represented in the RNA-seq datasets generated. The number in brackets represents the number of cell type-specific or process-specific genes identified in the previous dataset, and overlap is presented as a ratio out of 1.0 for differentiation expressed genes (DEG) up- or down-regulated in our dataset relative to intact samples. Asterisks represent a significant difference (p < 0.05) between the ratio of up- and down- regulated genes in a previously published transcriptome dataset compared to the ratio of all up- and down- regulated genes in our grafting dataset at a certain time point.

1237

1238

1239
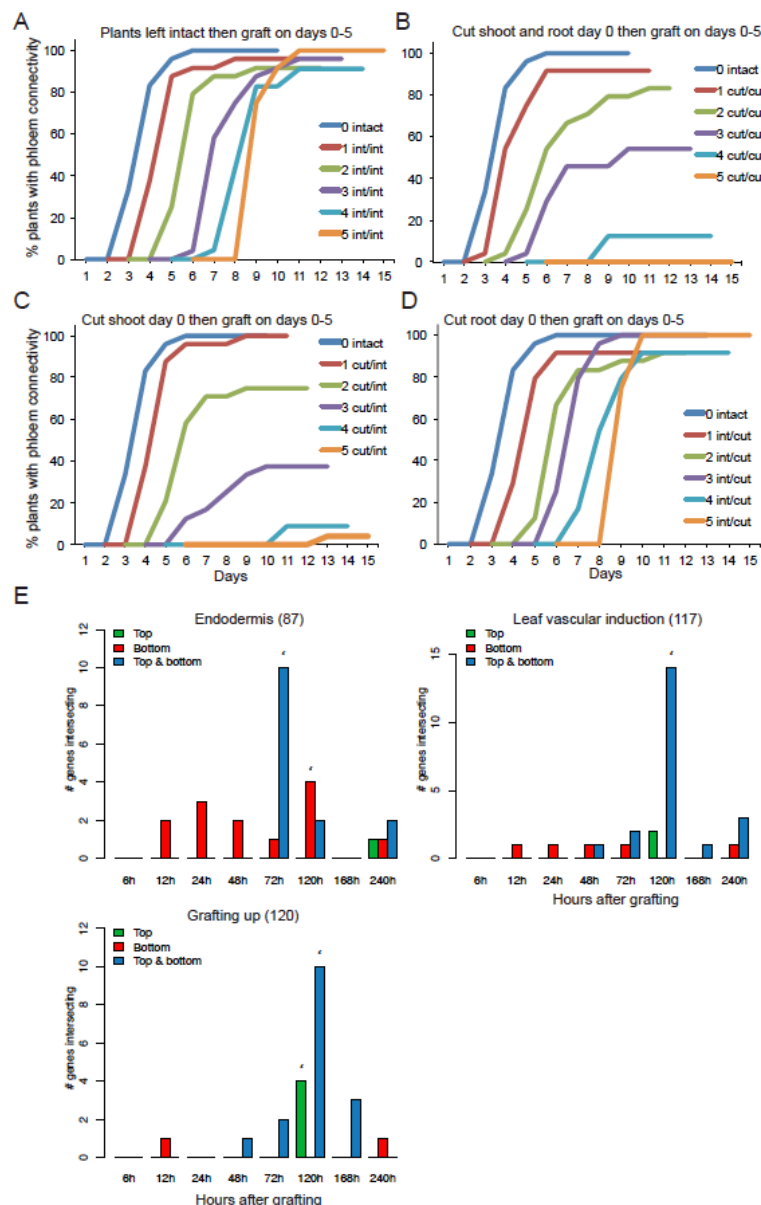
Figure S10. A subset of genes is differentially expressed only during graft formation, related to Figure 7. (A) *pSUC2::GFP* expressing *Arabidopsis* shoots were grafted to Col-0 wild type roots 0-5 days after transferring to grafting plates and kept intact until grafting (intact treatment). GFP movement to the roots for phloem connection assays was monitored over 7 days. (B) Plants were cut at day 0 and grafted at days 0-5 after cutting. (C) Shoots were cut at day 0 and grafted at days 0-5 after cutting. Roots were kept intact until immediately before grafting. (D) Roots were cut at day 0 and grafted at days 0-5 after cutting. Shoots were kept intact until immediately before grafting. (E) Genes differentially expressed in grafted tops and grafted bottoms show overlap with previously published genes whose transcripts are associated with the endodermis, vascular induction and grafting (see Table S1 for treatment information). Asterisks represent significant high overlap (p <0.05) of previously published gene sets that are also differentially expressed in the grafted samples at a certain time point.

1254